RADIATIVE AND TOPOLOGICAL PROPERTIES OF ONE-DIMENSIONAL ATOMIC CHAINS

A Thesis Submitted to
the Graduate School of
İzmir Institute of Technology
in Partial Fulfillment of the Requirements for the Degree of

MASTER OF SCIENCE

in Physics

by
Arda Deniz İYİCAN

July 2024

İZMİR

We approve the thesis of **Arda Deniz İYİCAN**

Examining Committee Members:

_____

Assoc. Prof. Dr. Özgür ÇAKIR
Department of Physics, İzmir Institute of Technology

_____

Prof. Dr. Ahmet Levent SUBAŞI
Department of Physics Engineering, İstanbul Technical University

_____

Assoc. Prof. Dr. Sevilay SEVİNÇLİ
Department of Photonics, İzmir Institute of Technology

_____

Assoc. Prof. Dr. Özgür ÇAKIR
Supervisor, Department of Physics
İzmir Institute of Technology

12 / July / 2024

_____

Prof. Dr. Lütfi ÖZYÜZER
Head of the Department of
Physics

_____

Prof. Dr. Mehtap EANES
Dean of the Graduate School

ACKNOWLEDGMENTS

ABSTRACT

RADIATIVE AND TOPOLOGICAL PROPERTIES
OF ONE-DIMENSIONAL ATOMIC CHAINS

In this thesis, the topological and vacuum-mediated collective properties of a one dimensional diatomic chain consisting of two identical two-level atoms per unit cell are examined. In the subspace where there is a fixed number of excitations on the chain, the system is described by a non-Hermitian effective Hamiltonian which takes the dissipative effects into account. In the presence of a single excitation on the chain, collective radiative behavior for an infinite chain is revealed from the complex energy bands corresponding to the effective Hamiltonian whose eigenstates are Bloch type states. For a finite chain with a single excitation, the radiative properties are revealed by the exact diagonalization of the effective Hamiltonian of the system. We identify the conditions for the existence of subradiant states. The considered model is an extended, non Hermitian SSH model due to mediated long range interactions and dissipation. For this system, we calculate the complex Berry phase to reveal the topological properties, then we identify the edge states for the topologically non-trivial cases. Furthermore, radiation patterns from radiant, subradiant and topological edge states are shown by computing the Poynting vector in the radiation zone.

ÖZET

TEK BOYUTLU ATOMİK ZİNCİRLERİN IŞINIMSAL VE TOPOLOJİK ÖZELLİKLERİ

Bu tezde, bir boyutlu, her birim hücresinde iki özdeş iki seviyeli atom bulunan bir diatomik zincirin topolojik ve vakum aracılı kolektif özellikleri incelenmiştir. Zincir üzerinde sabit sayıda uyarılmanın olduğu altuzayda, sistem, dissipatif etkileri dikkate alan non-Hermityen bir efektif Hamiltonyen ile tanımlanmaktadır. Zincirde tek bir uyarım varlığında, sonsuz bir zincir için kolektif radyatif davranış, öz durumları Bloch tipi durumlar olan etkin Hamiltoniyene karşılık gelen karmaşık enerji bantlarından ortaya çıkarılmıştır.Tek bir uyarıma sahip sonlu bir zincir için radyatif özellikler, sistemin etkin Hamiltonyeninin tam diyagonalizasyonuyla ortaya çıkarılmıştır. Altışınımlı durumların varlık koşulları belirlenmiştir. Ele alınan model, uzun menzilli etkileşimler ve dissipasyon nedeniyle genişletilmiş, non-Hermityen bir SSH modelidir. Bu sistem için topolojik özellikleri ortaya çıkarmak amacıyla kompleks Berry fazı hesaplanmış ve ardından topolojik olarak trivial olmayan durumlar için kenar durumları belirlenmiştir. Ayrıca, ışınımlı, altışınımlı ve topolojik kenar durumlarından gelen radyasyon desenleri, radyasyon bölgesindeki Poynting vektörünün hesaplanmasıyla gösterilmiştir.

TABLE OF CONTENTS

LIST OF FIGURES

CHAPTER 1

INTRODUCTION

A system of closely spaced atoms sharing a common environment is known to decay collectively with a rate larger or smaller than that of an individual atom. This phenomenon was first pointed out by Dicke in his seminal work showing the enhanced spontaneous emission for a gas of emitters confined to a container with dimensions smaller than the radiation wavelength and referred to such states as *superradiant states* of the gas.[1–3] The innate counterpart of these states are the ones that are formed due to destructive interatomic interference, leading to a reduced collective decay rate, are the *subradiant states*.[4] A stimulating work of Ficek and Tanaś proposed to exploit subradiance to achieve decoherence-free two-atom entangled state without isolating the two-atom system from the environment.[5] Ordered lattices of emitters allow collective effects to survive outside the Dicke regime.[6,7] Their subradiant behavior offers many practical applications such as efficient photon storage,[8–11] high reflectivity atomic mirrors[12] and atomic clocks[13] with enhanced stability. 1D arrays of atoms can also be employed as atomic waveguides, where the subradiant states serve as guided modes by prohibiting decay into free space.[14] Collective dynamics are also being studied in the context of waveguide QED, since waveguide mediated interactions between emitters survive beyond subwavelength limit.[15–18]

Topologically non-trivial systems are of interest due to their accommodation to implementing efficient quantum technologies such as single photon generation with enhanced indistinguishability,[19] fast and robust quantum-state transfer.[20,21] Diatomic 1D arrays with mediated interactions differ from the standard Su–Schrieffer–Heeger (SSH) model[22] by inherent long-range interactions within the chain and non-Hermiticity due to dissipation. In such non-Hermitian models, the adiabatic connection can be determined using the complex Berry phase calculated on a biorthogonal basis, serving as a topological invariant.[23]

1.1 Time Evolution for Closed Systems

It is known from the fundamental postulates of quantum mechanics that a pure state of a system isolated from its environment evolves according to the time-dependent Schrödinger Equation, and its time evolution is reversible. Namely, the time evolution of such states can be described by a unitary operator U such that,

$$i\hbar\frac{d}{dt}|\Psi(t)\rangle = H|\Psi(t)\rangle \quad \longrightarrow \quad |\Psi(t)\rangle = U|\Psi(0)\rangle, \qquad U = e^{-\frac{i}{\hbar}Ht}$$

Here, time evolution operator is defined in Schrödinger picture and for time independent Hamiltonians, which is the case for isolated systems. The conjugate transpose of the time evolution operator is its inverse, such that; $U^\dagger(t)U(t) = \mathbb{1}$ as long as the Hamiltonian is a Hermitian operator. This is always the case for closed systems, where the probability $\langle\Psi(t)|\Psi(t)\rangle$ is conserved throughout the time evolution. This can be easily generalized for the mixed states using density operators;

$$\rho = \sum_i p_i |\Psi_i\rangle\langle\Psi_i| \tag{1.1}$$

Where, p_i are the probabilities of the system to be found in state $|\Psi_i\rangle$. The evolution of the pure states $\{|\Psi_i\rangle\} \in \mathcal{H}$ in Schrödinger picture is defined by the unitary operator $U = e^{-\frac{i}{\hbar}Ht}$. Therefore, in Schrödinger picture, $\rho(t)$ can be found as:

$$\rho(t) = \sum_i p_i\, U|\Psi_i\rangle\langle\Psi_i|\,U^\dagger = U\rho\,U^\dagger \tag{1.2}$$

Differentiating by t gives us the Schrödinger picture **von Neumann equation** as follows;

$$\dot{\rho}(t) = \frac{1}{i\,\hbar}[H, \rho(t)] \tag{1.3}$$

Where $[\bullet, \bullet]$ is the commutator such that $[H, \rho(t)] = HU\rho U^\dagger - U\rho U^\dagger H$, and we exploited the fact that $[H, U^\dagger] = 0$.

1.2 Open System Dynamics

Time evolution for a system interacting with its surroundings is no longer a reversible process due to vulnerability to phenomena like dissipation and decoherence. Apart from Section 1.1, the dynamics of an open system can neither be described by von Neumann equation nor be carried by a unitary operator, since conservation of probability is no longer ensured. In this section, I will discuss the master equation approach for a system interacting with a Markovian bath, and there also will be a short introductory discussion of quantum trajectories.
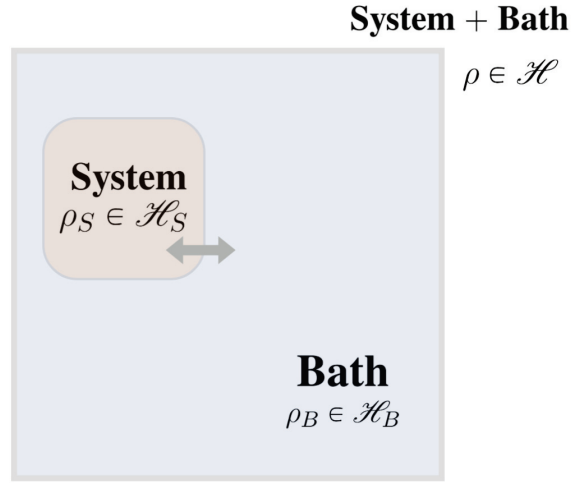
Figure 1.1: A schematic description of a closed composite system containing an open system of consideration and its environment. Its state ρ lives in in $\mathscr{H} = \mathscr{H}_S \otimes \mathscr{H}_B$.

To present the basis of what will be discussed about an open system, the situation to be considered is visualized in Figure 1.1. The open system lies in Hilbert space $\mathscr{H}_S$ and its time-dependent state is described by the density matrix $\rho_S(t)$. Similarly, for its environment, we have $\rho_B \in \mathscr{H}_B$, and for the total universe of system and bath, we have $\rho \in \mathscr{H} = \mathscr{H}_S \otimes \mathscr{H}_B$. The total Hamiltonian of this composite system, can be written as:

$$H_T = H_S \otimes \mathbf{1}_B + \mathbf{1}_S \otimes H_B + \mathcal{V}, \tag{1.4}$$

Here, H_S and H_B are the interaction-free Hamiltonians of the system and the bath respectively. And $\mathcal{V}$ is the interaction. Since the interaction Hamiltonian $\mathcal{V}$ operates on $\mathscr{H}_S \otimes \mathscr{H}_B$, without loss of generality, it can be decomposed into operators acting on the

two Hilbert spaces $\mathcal{H}_S$ and $\mathcal{H}_B$ as:

$$\mathcal{V} = \sum_\alpha A_\alpha \otimes B_\alpha \tag{1.5}$$

A_α and B_α are operators on the Hilbert space of the system $\mathcal{H}_S$ and the reservoir $\mathcal{H}_B$ respectively. This decomposition can be shown non rigorously by choosing complete orthonormal bases $\{|\varphi_i\rangle\}$ and $\{|\phi_j\rangle\}$ in $\mathcal{H}_S$ and $\mathcal{H}_B$. The set $\{|\varphi_i\rangle \otimes |\phi_i\rangle\}$ forms an orthonormal basis on $\mathcal{H}_S \otimes \mathcal{H}_B$. Then, we will have,

$$\mathcal{V} = \sum_{i,j\ k,l} \mathcal{V}_{i,j;k,l}(|\varphi_i\rangle\langle\varphi_k|) \otimes (|\phi_j\rangle\langle\phi_l|), \tag{1.6}$$

where we used the completeness relation for both subsystems. Here, $\mathcal{V}_{i,j;k,l}$ are the matrix elements of interaction term. $\mathcal{V}$ is already written as a linear combination of operators lying on each subspace, such that reshaping gives; $\mathcal{V} = \sum_\alpha c_\alpha A_\alpha \otimes B_\alpha$ where α runs over all possible combinations of indices. Lastly, we can redefine the operators absorbing the scalar coefficients c_α coming from matrix elements into either of them and obtain Equation (1.5). Having the total Hamiltonian and the description of considered system-environment setup, we can proceed delving into the dynamics of this system.

1.2.1   Gorini-Kossakowski-Sudarshan-Lindblad Master Equation

Gorini-Kossakowski-Sudarshan-Lindblad (GKSL) master equation describes the dynamics of an open system weakly coupled to a Markovian bath. To derive this, we begin by considering the total system-environment setup. The total universe consisting both of the environment and the system is closed and therefore, its time evolution is described by the von Neumann Equation (1.3). We begin solving the interaction picture von Neumann equation for $\rho \in \mathcal{H}_S \otimes \mathcal{H}_B$ by integrating both sides;

$$\rho(t) = \rho(0) - \frac{i}{\hbar} \int_0^t [H_I, \rho(t')]\, dt' \tag{1.7}$$

Differentiating again, with respect to time t, by using Von neumann equation for $\rho(t)$ again, we obtain an integro-differential equation:

$$\frac{d\rho(t)}{dt} = -\frac{i}{\hbar}[H_I, \rho(0)] - \frac{1}{\hbar^2} \int_0^t [H_I(t), [H_I(t'), \rho(t')]]dt' \qquad (1.8)$$

One more iteration gives a term which contains coupling constant of third order;

$$\frac{d\rho(t)}{dt} = -\frac{i}{\hbar}[H_I, \rho(0)] - \frac{1}{\hbar^2} \int_0^t [H_I(t), [H_I(t'), \rho(t)]]dt' + \mathcal{O}(g^3) \qquad (1.9)$$

And, further iterations will contain higher order coupling constants. In the realm of Born approximation, weak coupling limit, we can neglect $\mathcal{O}(g^3)$ and higher order terms. Further, we take Born approximation one step further and claim that, the system and bath remains separable at all times $\rho \approx \rho_S(t) \otimes \rho_B$. We could have also neglect higher order terms in Equation (1.9) under Born approximation beforehand by replacing $\rho_S(t')$ by $\rho_S(t)$ in Equation (1.8) assuming that the past does not effect the future of the system state which is consistent with markov approximation.[24] Lastly, since we are particularly interested in system dynamics, we trace out the reservoir degrees of freedom to obtain:

$$\frac{d\rho_S(t)}{dt} = -\frac{1}{\hbar^2} \int_0^t tr_B[H_I(t), [H_I(t'), \rho_s(t) \otimes \rho_B]]\,dt' \qquad (1.10)$$

Notice that we can choose that initially mean of B_α is zero $tr_B\{[H_I(t), \rho(0)]\} = 0$. In Equation (1.10), time evolution of density matrix depends on past times. In order to achieve a *memoryless* form, we substitute t' by $t - t'$ and set the upper limit of the integral to infinity. This is valid under Markovian approximation since the elapsed time for the system is much greater than the time for bath, for $t' \gg \tau_B$, making the integrand disappears fast.[24]

$$\frac{d\rho_S(t)}{dt} = -\frac{1}{\hbar^2} \int_0^\infty tr_B[H_I(t), [H_I(t - t'), \rho_s(t) \otimes \rho_B]]\,dt' \qquad (1.11)$$

Equation (1.11) is the Redfield equation.[25] It is Markovian as desired but does not guarantee the preservation of positivity of the density matrix.[26] Since negative properties are not physically acceptable, the map we provide should be completely positive and trace preserving. Positivity can be guaranteed by applying a secular approximation which is the well known rotating wave approximation in quantum optics. In order to do so, we first, decompose the Hermitian system operators $A_\alpha : \mathcal{H}_S \to \mathcal{H}_S$ forming the interaction

Hamiltonian in Equation (1.5).

$$A_\alpha(\omega) = \sum_{\epsilon'-\epsilon=\hbar\omega} P(\epsilon)\, A_\alpha\, P(\epsilon') \tag{1.12}$$

Where, the operator $P(\epsilon)$ projects onto the eigenstate with eigenvalue ϵ, and the index ω runs over all energy differences $\frac{1}{\hbar}(\epsilon' - \epsilon)$. The operators $A(\omega)$ are eigenoperators of superoperator $[H_S, \bullet]$ following;

$$
\begin{aligned}
[H_S, A_\alpha(\omega)] &= \sum_{\hbar\omega} H_S P(\epsilon) A_\alpha P(\epsilon') - \sum_{\hbar\omega} P(\epsilon) A_\alpha P(\epsilon') H_S \\
&= (\epsilon - \epsilon') \sum_{\epsilon'-\epsilon} P(\epsilon) A_\alpha P(\epsilon') = -\hbar\omega A_\alpha(\omega)
\end{aligned}
\tag{1.13}
$$

And,

$$[H_S, A_\alpha^\dagger(\omega)] = \hbar\omega A_\alpha^\dagger(\omega) \tag{1.14}$$

The time evolution of $A_\alpha(\omega)$ in interaction picture are found as;

$$e^{iH_S t} A_\alpha(\omega) e^{-iH_S t} = e^{-i\omega t} A_\alpha(\omega) \tag{1.15}$$

$$e^{iH_S t} A_\alpha^\dagger(\omega) e^{-iH_S t} = e^{i\omega t} A_\alpha^\dagger(\omega) \tag{1.16}$$

Giving $A_\alpha^\dagger(\omega) = A_\alpha(-\omega)$. The interaction picture interaction Hamiltonian is Hermitian and reads as:

$$H_I(t) = \sum_{\alpha,\omega} e^{-i\omega t} A_\alpha(\omega) \otimes B_\alpha(t) = \sum_{\alpha,\omega} e^{i\omega t} A_\alpha^\dagger(\omega) \otimes B_\alpha^\dagger(t) \tag{1.17}$$

Where, $B_\alpha(t) = e^{iH_B t} B_\alpha e^{-iH_B t}$. Recalling the Markovian Master Equation (1.11) for Equation (1.17), we have:

$$
\begin{aligned}
\dot\rho_S &= -\frac{1}{\hbar^2} \int_0^\infty tr_B\{H_I(t) H_I(t-t') \rho_S(t) \rho_B - H_I(t-t') \rho_S(t) \rho_B H_I(t) \\
&\qquad - H_I(t) \rho_S(t) \rho_B H_I(t-s) + \rho_S(t) \rho_B H_I(t-t') H_I(t)\}\, dt' \\
&= -\frac{1}{\hbar^2} \int_0^\infty tr_B\{H_I(t) H_I(t-t') \rho_S(t) \rho_B - H_I(t-t') \rho_S(t) \rho_B H_I(t)\}\, dt' + h.c.
\end{aligned}
\tag{1.18}
$$

Here, the tensor products are dropped for simplicity. Now we will substitute the interaction Hamiltonian in Equation (1.17). Since, H_I is Hermitian, we can use the first equality for $H_I(t - t') = \sum_{\beta,\omega} e^{-i\omega(t-t')} A_\beta(\omega) \otimes B_\beta(t - t')$ and the second one for $H_I(t) = \sum_{\alpha,\omega'} e^{i\omega't} A_\alpha^\dagger(\omega') \otimes B_\alpha^\dagger(t)$.

$$
\dot{\rho}_S = -\frac{1}{\hbar^2} \sum_{\omega,\omega';\alpha,\beta} \int_0^\infty dt' \, tr_B \{ e^{i\omega't} A_\alpha^\dagger(\omega') B_\alpha^\dagger(t) e^{-i\omega(t-t')} A_\beta(\omega) B_\beta(t - t') \rho_S(t) \rho_B
$$
$$
- e^{-i\omega(t-t')} A_\beta(\omega) B_\beta(t - t') \rho_S(t) \rho_B e^{i\omega't} A_\alpha^\dagger(\omega') B_\alpha^\dagger(t) \} + h.c.
$$
(1.19)

Simplifying this expression using the fact that system operators are not affected by the trace operation over bath degrees of freedom, and exploiting the cyclic property of trace, we obtain:

$$
\dot{\rho}_S = -\frac{1}{\hbar^2} \sum_{\omega,\omega';\alpha,\beta} \int_0^\infty dt' \, e^{-i(\omega-\omega')t} e^{i\omega t'} tr_B \{ B_\alpha^\dagger(t) B_\beta(t - t') \rho_B \}
$$
$$
\times \{ A_\alpha^\dagger(\omega') A_\beta(\omega) \rho_S(t) - A_\beta(\omega) \rho_S(t) A_\alpha^\dagger(\omega') \} + h.c.
$$
(1.20)

Where the expression;

$$
tr_B \{ B_\alpha(t) B_\beta(t - t') \} = \left\langle B_\alpha(t) B_\beta(t - t') \right\rangle
$$
(1.21)

are the bath correlation functions. And the remaining integral;

$$
\kappa_{\alpha\beta}(\omega) = \frac{1}{\hbar^2} \int_0^\infty e^{i\omega t'} \left\langle B_\alpha(t) B_\beta(t - t') \right\rangle dt'
$$
(1.22)

is spectral correlation tensor of the form:[24]

$$
\kappa_{\alpha\beta} = \frac{1}{2} \Gamma(\omega) + i\Omega(\omega)
$$
(1.23)

We can apply the rotating wave approximation by neglecting the fast oscillating terms $\omega \neq \omega'$ to obtain the following:

$$
\dot{\rho}_S = -\frac{1}{\hbar^2} \sum_{\omega,\omega';\alpha,\beta} \kappa_{\alpha\beta}(\omega) \{ A_\alpha^\dagger(\omega') A_\beta(\omega) \rho_S(t) - A_\beta(\omega) \rho_S(t) A_\alpha^\dagger(\omega') \} + h.c.
$$
(1.24)

Defining $\Gamma_{\alpha\beta} := \kappa_{\alpha\beta} + \kappa^*_{\alpha\beta}$, and $\Omega_{\alpha\beta} := \frac{-i}{2}(\kappa_{\alpha\beta} - \kappa^*_{\alpha\beta})$ we obtain GKSL master equation:

$$\dot{\rho}_S(t) = -\frac{i}{\hbar}[\mathcal{H}, \rho_S] + \mathscr{D}[\rho_S] \tag{1.25}$$

With the dissipator:

$$\mathscr{D}[\rho_S] = \sum_{\alpha,\beta} \Gamma_{\alpha\beta}(A_\alpha \rho_S A^\dagger_\beta - \frac{1}{2}\{A^\dagger_\beta A_\alpha, \rho_S\}) \tag{1.26}$$

This is also called the dissipator. and $\mathcal{H} = \hbar \sum_{\alpha,\beta} \Omega_{\alpha\beta} A^\dagger_\alpha A_\beta$ is the Hamiltonian with a Lamb shift correction. We can also put Equation (1.25) into a form referred to as Lindblad equation by diagonalizing the positive semi-definite matrix Γ by a unitary operator U;

$$U^\dagger \Gamma U = \Lambda \tag{1.27}$$

where Λ is a diagonal matrix with eigenvalues $\lambda_k \in \mathbb{R}_{\geqslant 0}$. Then, we can define L_k as;

$$L_k = \sum_\alpha U_{\alpha k} A_\alpha \tag{1.28}$$

Reshaping this way, we can write Equation (1.25) as:

$$\dot{\rho} = -\frac{i}{\hbar}[\mathcal{H}, \rho] + \sum_k \lambda_k (L_k \rho L^\dagger_k - \frac{1}{2}\{L^\dagger_k L_k, \rho\}) \tag{1.29}$$

which is the Lindblad master equation.

1.2.1.1 Quantum Trajectories

The quantum trajectory approach (also referred to as jump approach or Monte Carlo wave function method) describes the state of the system at a time as the sum of all possible trajectories. The idea is that the open system evolves continuously under a non Hermitian effective Hamiltonian in between sudden jumps.[27–29] To do so, we begin by

rewriting the GKSL Master Equation (1.25) in the form

$$\dot{\rho}(t) = \mathcal{L}\rho \tag{1.30}$$

Where the superoperator $\mathcal{L}$ is the generator of the time evolution with $\rho(t + \mathrm{d}t) \approx \rho(t) + \mathrm{d}t\mathcal{L}\rho(t)$. A formal solution to Equation (1.30) is;

$$\rho(t) = e^{\mathcal{L}\mathrm{t}}\rho(0) \tag{1.31}$$

Form of superoperator $\mathcal{L}$ is evident from Equation (1.25). And consists of the parts:

$$\mathcal{L}\bullet = \frac{i}{\hbar}[H, \bullet] + \sum_{\alpha,\beta}\Gamma_{\alpha\beta}(A_\alpha \bullet A_\beta^\dagger - \frac{1}{2}\{A_\beta^\dagger A_\alpha, \bullet\}) = \mathcal{L}_0 \bullet + \sum_{\alpha\beta}\mathcal{K}_{\alpha\beta}\bullet \tag{1.32}$$

With $\mathcal{L}_0\bullet = \frac{i}{\hbar}[H, \bullet]$ and $\mathcal{K}_{\alpha\beta}\bullet = \Gamma_{\alpha\beta}(A_\alpha \bullet A_\beta^\dagger - \frac{1}{2}\{A_\beta^\dagger A_\alpha, \bullet\})$. Without loss of generality, we can write Equation (1.31) in the following form (dropping the bullets for simplicity):

$$\rho(t) = e^{\{\mathcal{L}_0 + \sum_{\alpha\beta}[\mathcal{G}_{\alpha\beta} + (\mathcal{K}_{\alpha\beta} - \mathcal{G}_{\alpha\beta})]\}t}\rho(0) \tag{1.33}$$

With $\mathcal{G}_{\alpha\beta}[\bullet] = A_\alpha \bullet A_\beta^\dagger$. We can isolate the jump part by defining $S = e^{[\{\mathcal{L}_0 + \sum_{\alpha\beta}(\mathcal{K}_{\alpha\beta} - \mathcal{G}_{\alpha\beta})]\}t}$ Iterative solution gives a Dyson's series;

$$\rho(t) = \sum_{m=0}^{\infty}\int_0^t dt^{(m)}\dots\int_0^{t''} dt'[S(t - t^{(m)})(\sum_{n\alpha}\mathcal{G}_{\alpha\beta})S(t^{(m)} - t^{(m-1)}) \times \dots$$

$$\dots \times (\sum_{n\alpha}\mathcal{G}_{\alpha\beta})S(t')]\rho(0)$$

In time ordered form such that $t > t^{(m)} > t^{(m-1)} > \dots > t'' > t'$. This gives an expansion as follows:

$$\rho_S(t) = S(t)\rho(0) + \sum_{n\alpha}\left\{ \int_0^t dt' S(t - t')\mathcal{G}(S(t')\rho(0)) \right.$$

$$\left. + \int_0^t dt' S(t - t')\mathcal{G}(\int_0^{t'} dt'' S(t' - t'')\mathcal{G}(S(t'')\rho(0))) + \dots \right\}$$

Here, the jump operators $\mathcal{G}$ obviously represent the occurrence of instantaneous jumps in the system's state, while the continuous (but non-unitary) evolution in between successive

9

jumps is described by the superoperator S. Since the system evolves continuously under S, we can define operators $\mathcal{S}$ as:

$$S[\rho] = \mathcal{S}\rho\mathcal{S}^\dagger \tag{1.34}$$

Where $\mathcal{S} = e^{iH_{eff}t}$. The defined effective Hamiltonian H_{eff} is non Hermitian since in between jumps, the time evolution is still irreversible and therefore, $\mathcal{S}$ is not a unitary evolution operator. This effective Hamiltonian describing the continuous dynamics of the system is written as:

$$H_{eff} = \mathcal{H} - \frac{i\hbar}{2}\sum_{\alpha,\beta}\Gamma_{\alpha\beta}A_\alpha A_\beta^\dagger \tag{1.35}$$

We can also rewrite Equation (1.25) by separating the terms resposible for continuous evolution and jump terms in the dissipator with the non-Hermitian effective Hamiltonian H_{eff}:

$$\dot{\rho}_s = -\frac{i}{\hbar}(H_{eff}\rho_s - \rho_s H_{eff}^\dagger) + \sum_{\alpha,\beta}\Gamma_{\alpha\beta}\,A_\alpha\,\rho_s\,A_\beta^\dagger \tag{1.36}$$

1.2.2   Quantum Optical Master Equation

This section, leans on the simple situation when an atom is interacting with an external field. The overall Hamiltonian is again expressed as sum of uncoupled system Hamiltonian, free quantized field Hamiltonian and the interaction Hamiltonian.

$$H = H_S + H_B + H_I \tag{1.37}$$

Hamiltonian of the isolated two level atom is:

$$H_S = \frac{\hbar\omega_0}{2}\sigma_z \tag{1.38}$$

Where, ω_0 is the transition frequency, and $\sigma_z = |e\rangle\langle e| - |g\rangle\langle g| = \sigma_+\sigma_- - \sigma_-\sigma_+$ is well known Pauli z matrix. The environment is considered as 3D vacuum field. And the second quantized Hamiltonian of the multi mode field can be written in normal order by

choosing ground state energy zero as

$$H_B = \sum_{\vec{q},\nu} \hbar\omega_q b_\nu^\dagger b_\nu \tag{1.39}$$

Here, $\vec{q}$ is the wave vector with $q = \frac{\omega_q}{c}$, indices ν are over the field polarizations $\hat{e}_{1,2}$ and b, $b^\dagger$ are the annihilation and creation operators respectively. Lastly, the Hamiltonian for atom-field interaction can be written in dipole approximation as:

$$H_I = -\vec{d} \cdot \vec{E}(r) \tag{1.40}$$

where, $\vec{d}$ is the atomic dipole operator satisfying; $\vec{d} = \vec{\mu}\,|e\rangle\langle g| + \vec{\mu}^*\,|g\rangle\langle e| = \vec{\mu}\sigma_+ + \vec{\mu}^*\sigma_-$ with dipole moment $\vec{\mu} = \langle g|\,\vec{d}\,|e\rangle$ which is going to be considered real. The diagonal elements are zero, since the position operator (and therefore dipole operator) has odd parity. $\vec{E}$ is the external field at the position of the dipole. Such that;

$$\vec{E}(\vec{r}) = i \sum_{\vec{q},\nu} \sqrt{\frac{\hbar\omega_q}{2\varepsilon_0 V}} \hat{e}_{\vec{q}\nu} b_{\vec{q}\nu} e^{i(\vec{q}\cdot\vec{r})} + h.c. \tag{1.41}$$

By decomposing the interaction Hamiltonian in terms of bath and system related operators as in Equation (1.5), we have,

$$\vec{d}(t) = \sum_\omega e^{-i\omega t}\vec{A}(\omega) = \sum_\omega e^{i\omega t}\vec{A}^\dagger(\omega) \tag{1.42}$$

With that, and the interaction picture electric field, we write the interaction picture Hamiltonian as

$$H_I(t) = -\vec{d}(t) \cdot \vec{E}(t) = -\sum_\omega e^{-i\omega t}\vec{A}(\omega)\vec{E}(t) \tag{1.43}$$

We have $\left\langle \vec{E}(t) \right\rangle = tr_B\{\vec{E}(t)\rho_B\} = 0$ and the bath correlation functions introduces in Equation (1.21) are:

$$tr_B\{E_i(t)E_j(t - t')\} = \left\langle E_i(t)E_j(t - t') \right\rangle \tag{1.44}$$

where i, j run over cartesian coordinates. For ordinary vacuum, we have;

$$\langle 0|b_{\vec{q},\nu} b^{\dagger}_{\vec{q'},\nu'}|0\rangle = \delta_{k,k'} \delta_{\lambda,\lambda'}$$

$$\langle 0|b^{\dagger}_{\vec{q},\nu} b_{\vec{q'},\nu'}|0\rangle = 0$$

$$\langle 0|b_{\vec{q},\nu} b_{\vec{q'},\nu'}|0\rangle = 0 \tag{1.45}$$

$$\langle 0|b^{\dagger}_{\vec{q},\nu} b^{\dagger}_{\vec{q'},\nu'}|0\rangle = 0$$

Substitution into Equation (1.22) gives;

$$\kappa_{ij}(\omega) = \sum_{\vec{q},\nu} \frac{1}{\hbar^2} \left(\frac{\hbar\omega_k}{2\varepsilon_0 V} \right) \hat{e}^i_{\vec{q},\nu} \hat{e}^j_{\vec{q},\nu} \int_0^{\infty} dt' e^{-i(\omega_k - \omega)t'} \tag{1.46}$$

To go further, we can make use of the completeness relation for the polarization vectors;

$$\sum_{\lambda} \hat{e}^i_{\vec{q},\nu} \hat{e}^j_{\vec{q},\nu} = \delta_{ij} - \frac{k_i k_j}{|\vec{k}|^2} \tag{1.47}$$

Moreover, we apply the continuum limit to the summation over the wave vectors. For normalization length L, such that $L^3 = V$, we have, $q_i = \frac{2\pi n_i}{L}$, $dq_i = \frac{2\pi}{L} dn_i$. Hence; $d^3 q = (\frac{2\pi}{L})^3 d^3 n$. Therefore, we have;

$$\frac{1}{V} \sum_q \longrightarrow \int \frac{1}{V} d^3 n = \int \frac{V}{V} \frac{1}{(2\pi)^3} d^3 q = \frac{1}{(2\pi)^3} \int d^3 q \tag{1.48}$$

With the dispersion relation $\omega_q = cq$, and $d^3 q$ being $q^2 \sin\theta \, dq \, d\theta \, d\phi = q^2 dq \, d\Omega = \frac{\omega_q^2}{c^3} d\omega_q \, d\Omega$ in spherical coordinates. We can construct the integral as;

$$\frac{1}{V} \sum_q \longrightarrow \frac{1}{(2\pi)^3 c^3} \int_0^{\infty} d\omega_q \omega_q^2 \int d\Omega \tag{1.49}$$

Substituting this limit yields;

$$\kappa_{ij}(\omega) = \frac{1}{(2\pi)^3 c^3 \hbar^2} \int_0^{\infty} d\omega_q \omega_q^2 \int d\Omega \left(\frac{\hbar\omega_q}{2\varepsilon_0} \right) \left(\delta_{ij} - \frac{q_i q_j}{|\vec{q}|^2} \right) \int_0^{\infty} e^{-i(\omega_q - \omega)t'} dt' \tag{1.50}$$

The integration over solid angle results in [1];

$$\int d\Omega \left(\delta_{ij} - \frac{q_i q_j}{|\vec{q}|^2} \right) = \frac{8\pi}{3} \delta_{ij} \tag{1.51}$$

Moreover, From Sokhotski-Plemelj theorem,[27] the integral over t' takes the form;

$$\int_0^\infty dt' \, e^{-i(\omega_k - \omega)t'} = \pi\delta(\omega_k - \omega) - i\mathbb{P}\frac{1}{(\omega_k - \omega)} \tag{1.52}$$

Such That;

$$\begin{aligned}
\kappa_{ij}(\omega) = \kappa &= \frac{1}{2}\Gamma(\omega) + i\Omega(\omega) \\
&= \frac{1}{6\pi^2 c^3 \varepsilon_0 \hbar} \delta_{ij} \int_0^\infty d\omega_k \omega_k^3 \left(\pi\delta(\omega_k - \omega) - i\mathbb{P}\frac{1}{(\omega_k - \omega)} \right)
\end{aligned} \tag{1.53}$$

The term $\Omega(\omega)$ gives the renormalization to energy levels due to interaction with vacuum as a principal value integral, and $\Gamma(\omega)$ gives the single atom decay rate as:

$$\Gamma = \frac{\mu^2 \omega^3}{3\varepsilon_0 \pi c^3 \hbar} \tag{1.54}$$

Which is the spontaneous emission rate for a two level atom. Note that, the term $\mu^2 = \vec{d} \cdot \vec{d}$ did not naturally come from calculations. However, since μ is a constant scalar, we could have embedded its value into bath operators B instead of system operators and obtain μ^2 from bath correlation functions. Further, For $\vec{A}(\omega) = \sigma_-$, we have the Master Equation (1.25) in the form:

$$\dot{\rho}_s = \kappa(\sigma_-\rho_s(t)\sigma_+ - \sigma_+\sigma_-\rho_s(t)) + h.c. \tag{1.55}$$

---

[1]The integral is,

$$\int d\Omega \left(\delta_{ij} - \frac{q_i q_j}{|\vec{q}|^2} \right) = \int_0^\pi \int_0^{2\pi} \delta_{ij} \sin\theta \, d\theta \, d\phi - \int_0^\pi \int_0^{2\pi} \frac{q_i q_j}{|\vec{q}|^2} \sin\theta \, d\theta \, d\phi$$

The first Part of this integral gives $\int_0^\pi \int_0^{2\pi} \delta_{ij} \sin\theta \, d\theta \, d\phi = 4\pi\delta_{ij}$. and the second part gives for $\hat{q}_i = \frac{q_i}{q}$:

$$-\iint \hat{q}_i \hat{q}_j d\Omega = -\frac{4\pi}{3}\delta_{ij}$$

This is so, since the mean of components of unit vector in all directions is zero ($\bar{q}_i = \bar{q}_j = \bar{q}_q = 0$), and we have $\bar{q}_i^2 + \bar{q}_j^2 + \bar{q}_k^2 = 1$. The result of the integration can also be achieved by doing the integration for components of $\hat{q}$.

which is also called quantum optical master equation.

1.2.2.1   System Consisting Of N Atoms and Collective Effects

This section is a generalization of the previous discussion to more than one atom. The system, reservoir, and interaction Hamiltonians for this system are as follows:

$$H_s{}^{(n)} = \sum_{n=1}^{N} \frac{\hbar\omega_0^{(n)}}{2}\hat{\sigma}_z^{(n)}, \qquad H_B = \sum_{k,\lambda}\hbar\omega_k\hat{b}_\lambda^\dagger(k)\hat{b}_\lambda(k), \qquad H_I{}^{(n)} = -\sum_{n_1}^{N} d^{(n)} \cdot E(r^{(n)})$$

And the interaction Hamiltonian is;

$$H_I = -\sum_n\sum_\omega e^{-i\omega^{(n)}t}A^{(n)}(\omega) \cdot B^{(n)}(t) \tag{1.56}$$

where,

$$A^{(n)}(\omega) = \vec{\mu}^{(n)}\sigma_-^{(n)}, \qquad B^{(n)}(t) = E(r^n, t) \tag{1.57}$$

Yields, by the light of previous considerations;

$$\begin{aligned}\dot{\rho}_S &= \sum_{m,n}\kappa_{nm}(\sigma_-^{(n)}\rho_s(t)\sigma_+^{(m)} - \sigma_+^{(m)}\sigma_-^{(n)}\rho_s(t)) + h.c. \\ &= \sum_{m,n}\frac{1}{2}(\Gamma_{nm}(\omega) + i\Omega_{nm})(\omega)(\sigma_-^{(n)}\rho_s(t)\sigma_+^{(m)} - \sigma_+^{(m)}\sigma_-^{(n)}\rho_s(t)) + h.c.\end{aligned} \tag{1.58}$$

with,

$$\kappa_{ij}{}^{(nm)} = \frac{1}{2}\Gamma_{ij}^{nm}(\omega) + i\Omega_{ij}^{nm}(\omega)$$

And self interaction terms recover the previous result for single atom decay rate:

$$\Gamma_{ij}^{(nn)} = \Gamma_n = \frac{\mu^2\omega_0^{(n)3}}{3\varepsilon_0\pi c^3\hbar}$$

And for $n \neq m$, we need to solve,

$$\kappa_{ij}^{(nm)} = \int_0^\infty d\omega_k \frac{\omega_k^3}{16\pi\varepsilon_0 c^3 \hbar} M_{ij} \left(\pi\delta(\omega_k - \omega) - i\mathbb{P}\frac{1}{(\omega_k - \omega)} \right) \tag{1.59}$$

The M_{ij}'s are results of solid angle integration[2]. For ease of calculation, we assume that the dipole moments are parallel to each other. The result of this integration gives the collective decay rate $\Gamma(\vec{r}_{nm})$, and the coherent dipole-dipole interaction strength $\Omega(\mathbf{r}_{nm})$ as:[5]

$$\Gamma_{nm} = \frac{3\sqrt{\Gamma_n \Gamma_m}}{2} \left\{ C_1 \frac{\sin(k_0 r_{nm})}{k_0 r_{nm}} + C_2 \left[\frac{\cos(k_0 r_{nm})}{(k_0 r_{nm})^2} - \frac{\sin(k_0 r_{nm})}{(k_0 r_{nm})^3} \right] \right\} \tag{1.60}$$

and

$$\Omega_{nm} = \frac{3\sqrt{\Gamma_n \Gamma_m}}{4} \left\{ -C_1 \frac{\cos(k_0 r_{nm})}{k_0 r_{nm}} + C_2 \left[\frac{\sin(k_0 r_{nm})}{(k_0 r_{nm})^2} + \frac{\cos(k_0 r_{nm})}{(k_0 r_{nm})^3} \right] \right\} \tag{1.61}$$

Where, C_1 and C_2 are some constants determined depending on the cosine of the angle between the dipole moments, and the direction of the distance between the atoms ($|\vec{r}_{nm}| = |\vec{r}_m - \vec{r}_n| = |m - n|a$), such that for parallel dipoles; $C_1 = [1 - (\hat{\mu} \cdot \hat{r}_{nm})^2]$ and $C_2 = [1 - 3(\hat{\mu} \cdot \hat{r}_{nm}^2]$. Distance dependence of this collective parameters are demonstrated in Figure 1.2 for two identical atoms with dipole moments parallel to each other. Figure shows that the collective dynamics are mostly effective in the limit where the distance is less than half the wavelength and they damp as the distance increases. To investigate the dynamics of the system state, we can further exploit the discussions above. And we can write Equation (1.58) as (see Section 1.2.1.1):

$$\dot{\rho}_S = -i(H_{eff}\rho_s - \rho_s H_{eff}^\dagger) + \sum_{\substack{n,m \\ i,j}} \Gamma_{nm}\sigma_-^{(n)}\rho_s\sigma_+^{(m)} \tag{1.62}$$

where, the effective Hamiltonian is:

$$H_{eff} = \mathcal{H} - \frac{i}{2}\sum_{nm} \Gamma_{nm}\sigma_+^{(n)}\sigma_-^{(m)} \tag{1.63}$$

---

[2]For example, for two atoms M is the following matrix;

$$M = \begin{bmatrix} \frac{4\pi}{k^3 R^3}(kR\cos kR + (k^2 R^2 - 1)\sin kR) & 0 & 0 \\ 0 & \frac{4\pi}{k^3 R^3}(kR\cos kR + (k^2 R^2 - 1)\sin kR) & 0 \\ 0 & 0 & \frac{8\pi}{k^3 R^3}(\sin kR - kR\sin kR) \end{bmatrix}$$

15
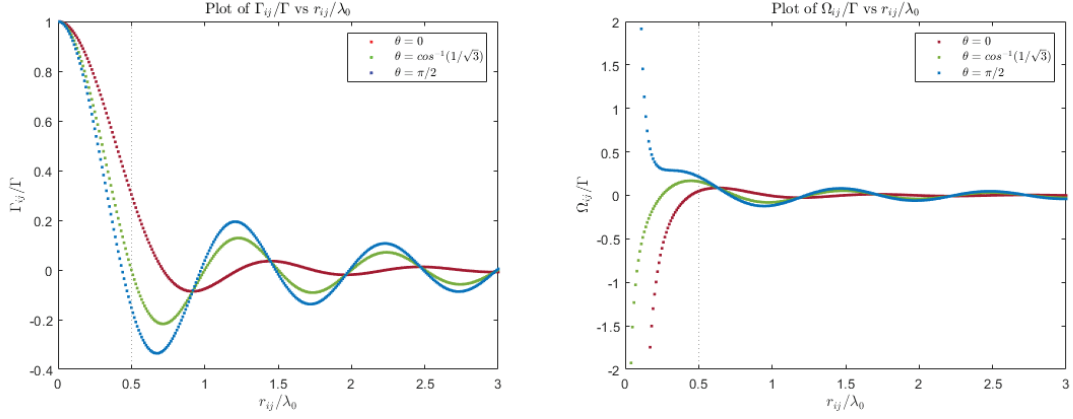
Figure 1.2: The collective parameters as functions of interatomic distance for two identical atoms with parallel dipole moments. $\hat{d} \cdot \hat{r}_{nm} = 1, 1/\sqrt{3}, 0$ are plotted in red, green, and blue, respectively. In left panel, vertical axis shows Γ_{nm}/Γ and in right panel, it shows Ω_{nm}/Γ where, Γ is decay rate of a single atom, in both plots, horizontal axis shows the ratio of interatomic distance to resonant wavelength (r_{nm}/λ_0).

And $\mathcal{H}$ is the system Hamiltonian with a Lamb Shift renormalization. It reads:

$$\mathcal{H} = \sum_{nm} \Omega_{nm} \sigma_+^{(m)} \sigma_-^{(n))} \tag{1.64}$$

1.3 Su–Schrieffer–Heeger Model

A dimerized one-dimensional lattice is energetically more stable than a monatomic chain with a band gap opening at Fermi level due to increased unit cell length. This phenomenon of the tendency of a regularly ordered chain to dimerize is called *the Peierls instability*.[30] In their pioneering work, W. P. Su, J. R. Schrieffer, and A. J. Heeger investigated the conductive properties of polyacetalyne which is an example of such structures.[22] The *SSH model* generally describes a closed one-dimensional diatomic system with nearest-neighbor hoppings,[31] as illustrated in Figure 1.3.

The model has the following tight binding Hamiltonian.

$$H = v \sum_{i=1}^{N} c_{A,i}^{\dagger} c_{B,i} + w \sum_{i=1}^{N-1} c_{A,i+1}^{\dagger} c_{B,i} + h.c. \tag{1.65}$$

Here, v is the intracell and w is intercell hopping amplitudes. And the two sublattices A and B are as shown in Figure 1.3. Switching to reciprocal space with the help of Fourier
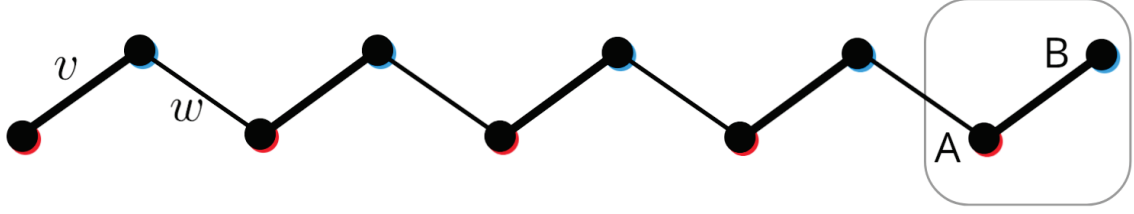
Figure 1.3: Schematic description of standard SSH model with staggered nearest neighbor hopping amplitudes v and w being hopping from sublattice A to B and from B to A respectively. Choice of a unit cell is always as shown in square which makes v and w the intracell and intercell hopping amplitudes respectively.

transform of annihilation operators:

$$a_k = \frac{1}{\sqrt{N}} \sum_{n=1}^{N} e^{-i\vec{k}\cdot n\vec{a}} c_{A,n}$$

$$b_k = \frac{1}{\sqrt{N}} \sum_{n=1}^{N} e^{-i\vec{k}\cdot n\vec{a}} c_{B,n}$$

With periodic boundary conditions, we have the bulk Hamiltonian:

$$H = v \sum_{k\in[-\pi,\pi]} a_k^\dagger b_k + b_k^\dagger a_k + w \sum_k e^{ika} a_k^\dagger b_k + e^{-ika} b_k^\dagger a_k = \sum_k \Psi_k^\dagger H(k) \Psi_k \quad (1.66)$$

With spinors $\Psi_k = \begin{pmatrix} a_k \\ b_k \end{pmatrix}$. Therefore, we have:

$$H(k) = \begin{pmatrix} 0 & v + we^{-ika} \\ v + we^{ika} & 0 \end{pmatrix} \quad (1.67)$$

This 2×2 Hamiltonian can be written in terms of Pauli matrices, as:

$$H(k) = \vec{\gamma}(k) \cdot \vec{\sigma} \quad (1.68)$$

The vector $\vec{\gamma}(k) = (v + w\cos(ka),\ w\sin(ka),\ 0)$ is closely related to topological invariant of the system. The winding of $\gamma(k)$ around the origin in a closed loop over k gives the topological invariant associated with the model of consideration.For the parametrization in Equation (1.68), the Berry's phase can be obtained as:

$$\Phi = \frac{1}{2} \int_{-\pi}^{\pi} \frac{\gamma(k)}{|\gamma(k)|^2} \times \frac{d}{dk} \gamma(k) dk = \frac{1}{2} \int_{-\pi}^{\pi} \frac{d\varphi(k)}{dk} dk = \pi W \quad (1.69)$$
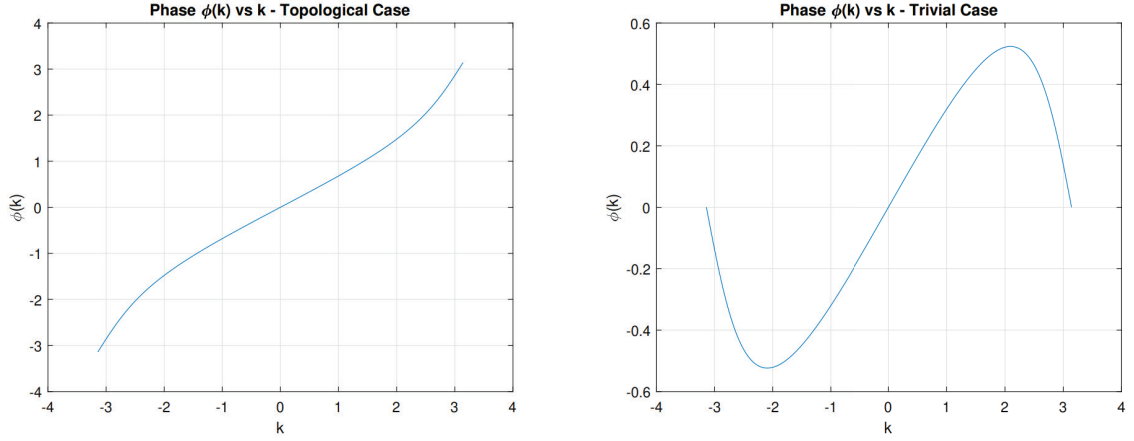
Figure 1.4: The phase $\varphi(k) = arg(\gamma_x(k)) + i\gamma_y(k))$ for $v < w$ (left) and $v > w$ (right).

Where $\varphi(k) = arg(\gamma_x(k)) + i\gamma_y(k))$. This phase φ is plotted in Figure 1.4 for $v > w$ and $v < w$. In the left panel of the figure ($v < w$), the phase φ increases without returning to its original point. This makes the integral in Equation (1.69) over closed path nonzero. Therefore, this corresponds to the topologically non-trivial case. On the right panel, $v > w$ and the angle ϕ returns to its initial point over a closed loop, making the Berry phase 0.
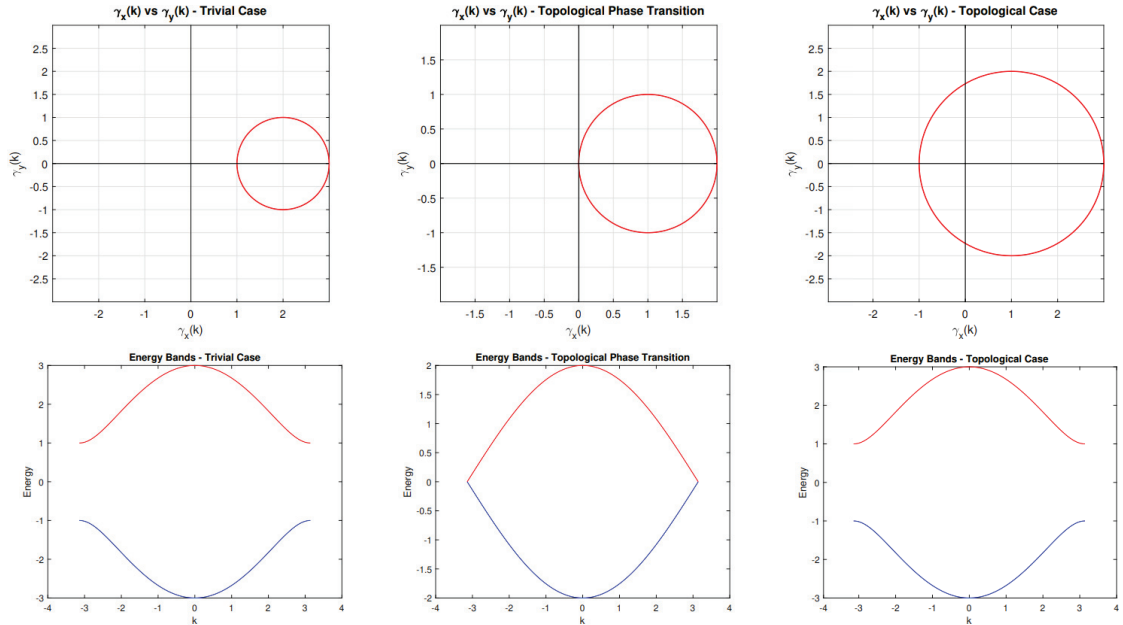
Figure 1.5: The winding of $\vec{\gamma}(k)$ are shown in upper panel and the band diagrams of the SSH chain are plotted in lower panel. From left to right, we have $v > w$, $v = w$, $v < w$ respectively.

In Equation (1.69), W is called the *winding number* and represents the number of windings of $\vec{\gamma}(k)$ around the origin in a closed loop. φ will be the angle that $\vec{\gamma}(k)$ makes with its vertical axis. The windings and band diagrams for different intercell/intracell hoppings are shown in Figure 1.5. For $v < w$, the origin is enclosed by the closed path of $\gamma(k)$ with $W = 1$ making the system topologically non-trivial. For $v > w$, we have a topologically trivial system with $W = 0$. Note that band closing occurs at $w = v$ making the topological invariant undefined, This is the topological phase transition point.

CHAPTER 2

THE MODEL AND RESULTS

This chapter leans on a particular model. The atomic system of consideration will be a singly excited one-dimensional diatomic chain, and the environment will be again a three-dimensional vacuum. The detailed description of the model is presented in Section 2.2. Although some relevant calculations were done in the previous chapter, for the sake of completeness, some steps will be briefly introduced again without diving into details that are already discussed. Before introducing the diatomic model, as an example, collective dynamics of an infinite monatomic chain will be discussed in Section 2.1.

2.1 Collective Dynamics of Infinite Monatomic Chain

This section leans on the particular example of a one-dimensional singly excited infinite monatomic chain. The chain consists of equally spaced, identical, two-level atoms with dipole moments parallel to each other. Introducing one excitation to the infinite system such that the Bloch states read:

$$|\Psi_{sys}(k)\rangle = \sum_n e^{ikna} c_n |n\rangle \tag{2.1}$$

Where $|n\rangle = \sigma_+^n |g\rangle$ indicates that one excitation is in n^{th} atom while all other atoms are in ground state. And, the effective bulk Hamiltonian obeys;

$$H_{eff}(k) |\Psi_{sys}(k)\rangle = E_k |\Psi_{sys}(k)\rangle \tag{2.2}$$

We have, in real space, $H_{eff} = \sum_{nm} (\Omega_{nm} - \frac{i}{2}\Gamma_{nm})\sigma_+^n \sigma_-^m$ where n, m indicates atoms. Since $\sigma_+^n \sigma_-^m |\Psi_{sys}(k)\rangle = e^{ikma}\sigma_+^n |g\rangle$, and we can substitute it to obtain coherent and

dissipative interactions as follows:

$$\Omega_k = \sum_{n,m} e^{ik(n-m)a}\Omega_{nm} \tag{2.3a}$$

$$\Gamma_k = \sum_{n,m} e^{ik(n-m)a}\Gamma_{nm} \tag{2.3b}$$

Where the real space collective parameters are as in Equations (1.60) and (1.61). Then we have the Green's function in reciprocal space:

$$G_k = \Omega_k - \frac{i}{2}\Gamma_k \tag{2.4a}$$

Giving complex energies E_k with Equation (2.2) of the from :

$$E_k = G_k = \frac{3\Gamma}{4}\sum_{n,m} e^{-i(k-k_0)r_{nm}}\{-C_1\frac{1}{(k_0 r_{nm})} + C_2(\frac{-i}{(k_0 r_{nm})^2} + \frac{1}{(k_0 r_{nm})^3})\} \tag{2.5}$$

Again, $C_1 = [1 - (\hat{\mu}\cdot\hat{r}_{nm})^2]$ and $C_2 = [1 - 3(\hat{\mu}\cdot\hat{r}_{nm}^2)]$. The real part E_k gives the dispersion, and the imaginary part gives the collective decay rate. This example model shows collective subradiant behavior when the atomic spacings a is smaller than half the resonant wavelength as can be seen in Figure 2.1. The figure shows decay rates and dispersions in first Brillouin zone for parallel dipoles. In the first panel of the figure, the interatomic spacing a lies within the discussed critical region such that $a = 0.4\lambda_0 < 0.5\lambda_0$. And we can observe completely subradiant modes for $|k| > |k_0|$. However, this single
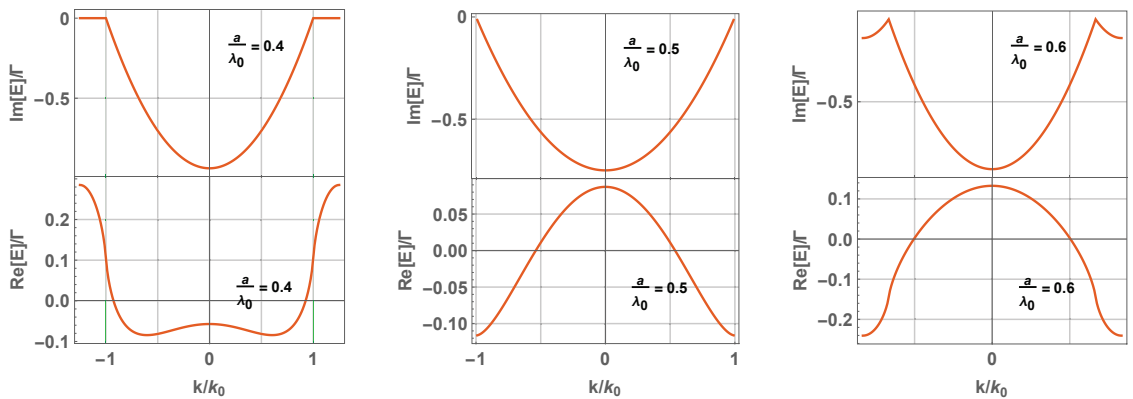
Figure 2.1: Real (lower panel) and imaginary (upper panel) bands are plotted for $\vec{d}\parallel\vec{r}$. columns show different lattice parameters $a = 0.4\lambda_0, 0.5\lambda_0, 0.6\lambda_0$ from left to right. Green lines which only lie on first Brillouin zone when $a < 0.5\lambda_0$ are the light lines ($k = \pm k_0$).

band example is not suitable for investigating the topological properties since we cannot define a topological invariant ensuring protected edge/surface states for such models.

2.2 Description of The Diatomic Model

The discussions in the following sections will all be about a singly excited one-dimensional diatomic chain immersed in a 3D vacuum field. The two level atoms forming the chain are all identical and separated by alternating spacings. The chain is illustrated in Figure 2.2. Here, all atoms have natural frequencies ω_0 when isolated, The unit cell length is indicated by a, and the interatomic distance within a unit cell is denoted by b. This model can be considered as an extended non Hermitian SSH model.

$$\vec{r}_{nA} = na\,\hat{z}$$
$$\vec{r}_{nB} = na + b\,\hat{z}$$
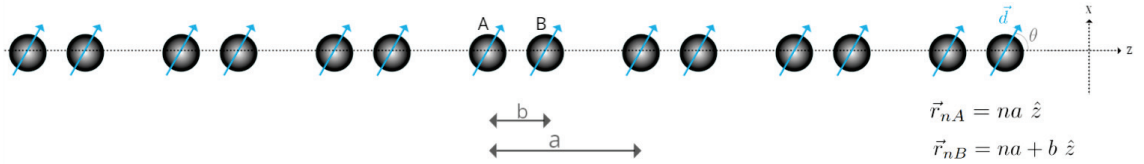
Figure 2.2: Schematic of the atomic system.

The model Hamiltonian, again, consists of the uncoupled atomic system Hamiltonian H_A, Hamiltonian of the bath H_B and interaction Hamiltonian H_I.

$$H = H_S + H_B + H_I \tag{2.6}$$

Total Hamiltonian of the atomic system can be written under dipole approximation as:

$$H = H_S + H_B + H_I = \sum_{n\alpha} \frac{\hbar\omega_0^{n\alpha}}{2}\sigma_z^{n\alpha} + \sum_{\vec{q},\nu} \hbar\omega_q b_\nu^\dagger(\vec{q})b_\nu(\vec{q}) - \sum_{n\alpha} \vec{d}^{\,n\alpha} \cdot \vec{E}(\vec{r}_{n\alpha}) \tag{2.7}$$

Where, the index n runs through all unit cells, and α runs through the two sublattices A and B. Here, $\vec{d}^{\,n\alpha}$ is the dipole operator for the atom at unit cell n and sublattice α and $\vec{E}(\vec{r}_{n\alpha})$ is the external field at the position of the dipole. Such that;

$$H_I = -\sum_{n\alpha} \vec{d}^{\,n\alpha} \cdot \vec{E} = -\sum_{\substack{q,\nu \\ n,\alpha}} g_{q\nu}^{n\alpha}(e^{i\vec{q}\cdot\vec{r}_{n\alpha}}\sigma_+^{n\alpha}b_{q\nu} + h.c) \tag{2.8}$$

22

Where $g_{q\nu}^{n\alpha} = \vec{d}^{n\alpha} \cdot \mathbf{e}_{q\nu}\sqrt{\frac{\hbar\omega_q}{2\varepsilon_0 V}} = \vec{d} \cdot \mathbf{e}_{q\nu}\sqrt{\frac{\hbar\omega_q}{2\varepsilon_0 V}} = g_{q\nu}$ for identical atoms with parallel dipole moments. Giving the total Hamiltonian in Schrödinger picture:

$$H = \sum_{n\alpha} \frac{\hbar\omega_0}{2}\sigma_z^{n\alpha} + \sum_{q\nu} \hbar\omega_q b_{q\nu}^\dagger b_{q\nu} - \sum_{\substack{q,\nu \\ n,\alpha}} g_{q\nu}(e^{i\vec{q}\cdot\vec{R}^{n\alpha}}\sigma_+^{n\alpha}b_{q\nu} + h.c). \tag{2.9}$$

It can be seen from previous sections that the dynamics of the atomic chain can be described by the following quantum optical master equation:

$$\dot{\rho}_S = \sum_{\substack{n,m \\ \alpha,\beta}} \kappa_{n\alpha;m\beta}(\sigma_-^{n\alpha}\rho_S(t)\sigma_+^{m\beta} - \sigma_+^{m\beta}\sigma_-^{n\alpha}\rho_S(t)) + h.c. \tag{2.10}$$

Where, $\kappa_{n\alpha;m\beta}$ is the one-sided Fourier transform of bath correlation functions, defined as

$$\kappa_{n\alpha;m\beta} = \frac{|\mu|^2}{\hbar^2}\int_0^\infty dt' e^{i\omega^{n\alpha}t'}\langle E^{m\beta}(t)E^{n\alpha}(t-t')\rangle = \frac{1}{2}\Gamma_{n\alpha;m\beta} + i\Omega_{n\alpha;m\beta} \tag{2.11}$$

Collective atomic parameters $\Gamma_{n\alpha;m\beta} = \kappa_{n\alpha;m\beta} + \kappa_{n\alpha;m\beta}^*$, and $\Omega_{n\alpha;m\beta} = -\frac{i}{2}(\kappa_{n\alpha;m\beta} - \kappa_{n\alpha;m\beta}^*)$ are respectively, related to collective decay rate, and coherent dipole-dipole interaction due to coupling between atoms through the reservoir. After the calculation of Equation (2.11) for vacuum field, they are found to be as follows:

$$\Gamma_{n\alpha;m\beta} = \frac{3\Gamma}{2}\left\{C_1\frac{\sin(k_0 r_{n\alpha;m\beta})}{k_0 r_{n\alpha;m\beta}} + C_2\left[\frac{\cos(k_0 r_{n\alpha;m\beta})}{(k_0 r_{n\alpha;m\beta})^2} - \frac{\sin(k_0 r_{n\alpha;m\beta})}{(k_0 r_{n\alpha;m\beta})^3}\right]\right\} \tag{2.12}$$

and

$$\Omega_{n\alpha;m\beta} = \frac{3\Gamma}{4}\left\{-C_1\frac{\cos(k_0 r_{n\alpha;m\beta})}{k_0 r_{n\alpha;m\beta}} + C_2\left[\frac{\sin(k_0 r_{n\alpha;m\beta})}{(k_0 r_{n\alpha;m\beta})^2} + \frac{\cos(k_0 r_{n\alpha;m\beta})}{(k_0 r_{n\alpha;m\beta})^3}\right]\right\} \tag{2.13}$$

Where, Γ is the spontaneous emission rate of an individual atom, which is the same for all identical atoms forming the chain. C_1 and C_2 are some constants determined depending on the cosine of the angle between the dipole moment, and the direction of the chain, such that; $C_1 = [1 - (\hat{\mu} \cdot \hat{r}_{n\alpha;m\beta})^2]$ and $C_2 = [1 - 3(\hat{\mu} \cdot \hat{r}_{n\alpha;m\beta})^2]$. The Master Equation (2.10) can be rewritten in the Lindblad form as,

$$\dot{\rho}_s = -i[\mathcal{H}, \rho_s(t)] + \mathscr{D}(\rho_s(t)) \tag{2.14}$$

23

with dissipator,

$$\mathscr{D}(\rho_s(t)) = \sum_{\substack{n,m \\ \alpha,\beta}} \Gamma_{n\alpha;m\beta} \sigma_-^{n\alpha} \rho_s \sigma_+^{m\beta} - \frac{1}{2} \Big\{ \sum_{\substack{n,m \\ \alpha,\beta}} \Gamma_{n\alpha;m\beta} \sigma_+^{m\beta} \sigma_-^{n\alpha}, \rho_s \Big\} \tag{2.15}$$

$\mathcal{H}$ is the renormalization of uncoupled system Hamiltonian H_S with a Lamb shift-like correction.

$$\mathcal{H} = \sum_{\substack{n,m \\ \alpha,\beta}} \Omega^{n\alpha;m\beta} \sigma_+^{m\beta} \sigma_-^{n\alpha} \tag{2.16}$$

Further, We can separate the continuous(jump free) non-unitary dissipation terms and the jump term in Equation (2.15) and rewrite the master equation by defining a non-Hermitian effective Hamiltonian for the system dynamics.

$$\dot{\rho}_s = -\frac{i}{\hbar}(H_{eff}\rho_s - \rho_s H_{eff}^\dagger) + \sum_{\substack{n,m \\ \alpha,\beta}} \Gamma_{n\alpha;m\beta} \sigma_-^{n\alpha} \rho_s \sigma_+^{m\beta} \tag{2.17}$$

With non-Hermitian effective Hamiltonian,

$$H_{eff} = H_{LS} - \frac{i}{2} \sum_{\substack{n,m \\ \alpha,\beta}} \Gamma_{n\alpha;m\beta} \sigma_+^{n\alpha} \sigma_-^{m\beta} = -i \sum_{\substack{n,m \\ \alpha,\beta}} \kappa_{n\alpha;m\beta} \sigma_+^{n\alpha} \sigma_-^{m\beta} \tag{2.18}$$

You may find more discussion about this step in Section 1.2.1.1. Here $\mathcal{H}$ generates coherent unitary dynamics, and non-unitary of evolution comes from the non-Hermiticity of H_{eff} due to the second part with dissipative rate $\Gamma_{n\alpha;m\beta}$, and $\kappa_{n\alpha;m\beta}$ is defined in Equation (2.11) in reciprocal space, for infinite diatomic chain, the corresponding ansatz wavefunction will be of the form;

$$|\Psi_k\rangle = c_A \left| \Psi_k^A \right\rangle + c_B \left| \Psi_k^B \right\rangle \tag{2.19}$$

With,

$$|\Psi_k^\alpha\rangle = \sum_n e^{ikna} \sigma_+^{(n\alpha)} |g\rangle \tag{2.20}$$

Satisfying, Schrödinger equation for the effective Hamiltonian:

$$H_{eff} \begin{pmatrix} c_A \\ c_B \end{pmatrix} = E_{\pm} \begin{pmatrix} c_A \\ c_B \end{pmatrix} \tag{2.21}$$

Since we have $\sigma_+^{(m)} \sigma_-^{(n)} |\Psi_k\rangle = e^{-ikr_{nm}} |\Psi_k\rangle$ we have the Green's functions $G_{\alpha;\beta}(k) = -i\kappa_{\alpha;\beta}(k) = \Omega_{\alpha;\beta}(k) - \frac{i}{2}\Gamma_{\alpha;\beta}(k)$ as:

$$\begin{aligned} G_{AA}(k) = G_{BB}(k) = G_{\alpha\alpha} = \frac{3\Gamma}{4} \sum_{n,m} e^{-i(k-k_0)r_{nm}} & \left\{ -C_1 \frac{1}{(k_0 r_{nm})} \right. \\ & \left. + C_2 \left[\frac{-i}{(k_0 r_{nm})^2} + \frac{1}{(k_0 r_{nm})^3} \right] \right\} \end{aligned} \tag{2.22a}$$

$$\begin{aligned} G_{AB}(k) = \sum_{n,m} \frac{3\Gamma}{4} e^{-ikr_{nm}} e^{ik_0|r_{nm}+b|} & \left\{ -C_1 \frac{1}{k_0|r_{nm}+b|} \right. \\ & \left. + C_2 \left[\frac{-i}{k_0^2|r_{nm}+b|^2} + \frac{1}{k_0^3|r_{nm}+b|^3} \right] \right\} \end{aligned} \tag{2.22b}$$

$$\begin{aligned} G_{BA}(k) = \sum_{n,m} \frac{3\Gamma}{4} e^{-ikr_{nm}} e^{ik_0|r_{nm}-b|} & \left\{ -c_1 \frac{1}{k_0|r_{nm}-b|} \right. \\ & \left. + C_2 \left[\frac{-i}{k_0^2|r_{nm}-b|^2} + \frac{1}{k_0^3|r_{nm}-b|^3} \right] \right\} \end{aligned} \tag{2.22c}$$

Where, for the hoppings between same sublattices $G_{\alpha\alpha}$, Equation (2.22a) is the same as that of a monatomic chain which is shown in Equation (2.5). We therefore have, for the effective Hamiltonian $H_{eff}(k) = \sum_{\alpha\beta} G_{\alpha\beta}(k)\sigma_+^\alpha \sigma_-^\beta$, the following energies;

$$E_{\pm} = G_{\alpha\alpha} \pm \sqrt{G_{(\alpha\beta)}G_{(\beta\alpha)}} \tag{2.23}$$

2.3 Subradiant Behavior

When an atomic system interacts with its surroundings, the atoms forming the chain become mutually coupled to the environment, leading to interatomic correlations mediated by interactions with a common field. And the information is kept in the chain rather than the individual atoms. This results in a *collective* photon emission. The wavefunctions of the atomic chain are superpositions of the different atomic states and due

constructive/destructive quantum interference between these atomic states the collective decay rate may be enhanced/reduced relative to that of an independent atom leading to occurrence of *superradiance/subradiance*.[1]

The discussions in this section will be based on the collective decay rates $2\Im[E]$ for different states of the system in the single excitation framework. Where E's are the complex eigenvalues that corresponds to the considered eigenstate of non Hermitian effective Hamiltonian of the atomic chain. For infinite chain, I will refer to the states as *subradiant* when the decay rates $\Im[E_k]$ become zero for some modes. However, for a finite chain, the boundaries of the chain prevent an excitation from having an infinite lifetime. Therefore, I will refer to states that have much smaller decay rates than that of an individual atom, such that $\Im[E] \ll 0.5\,\Gamma$ as *subradiant*.

2.3.1 Infinite Diatomic Chain

Similar to the monatomic case, as discussed in Section 2.2, we have the bloch states in reciprocal space (see Equation (2.19)):

$$|\Psi_k\rangle = c_A \left|\Psi_k^A\right\rangle + c_B \left|\Psi_k^B\right\rangle = \frac{1}{\sqrt{N}} \sum_{n,\alpha} e^{ikna} c_\alpha \left|n_\alpha\right\rangle \tag{2.24}$$

And, the effective Hamiltonian $H_{eff} = \sum_{\substack{n,m \\ \alpha,\beta}} G_{n\alpha;m\beta}(k)\sigma_+^{n\alpha}\sigma_-^{m\beta}$ becomes.

$$H_{eff}(k) = \begin{pmatrix} G_{AA}(k) & G_{AB}(k) \\ G_{BA}(k) & G_{BB}(k) \end{pmatrix} \tag{2.25}$$

The Green functions are as given in Equation (2.22). They are all complex, and $G_{AB}(k) \neq G_{BA}^*(k)$. And $E_\pm(k) = G_{AA} \pm \sqrt{G_{AB}\,G_{BA}}$. The real and imaginary parts of $E_\pm(k)$ for different lattice parameters are plotted in Figure 2.3. As in Figure 2.1, the real parts give the dispersion while the imaginary parts give the decay rates for the corresponding modes.

As can be seen in top row of Figure 2.3, for $a = 0.4\,\lambda_0$, we observe a subradiant regime outside the region enclosed by the light line $k = \pm k_0$, namely outside $-k_0 < k < k_0$, where the decay rates of all modes diminish. This means that the excitation stays in the chain and do not decay into free space. At $a = 0.5\lambda_0$, the imaginary parts of $E_\pm(k)$ touch at the two end of first Brillouin zone. And lastly, there is no subradiant behavior performed by the chain observed since the imaginary parts of the complex energies never become zero when the lattice parameter is greater than half the transition wavelength ($a > 0.5\lambda_0$).
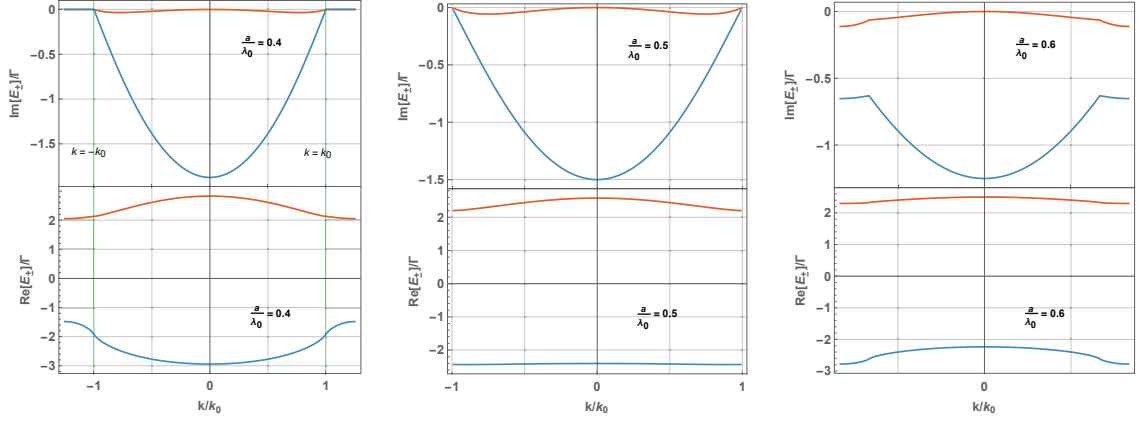
Figure 2.3: The band diagrams for real (bottom) and imaginary (top) parts of energies for different lattice parameters ($a = 0.4\lambda_0$, $0.5\lambda_0$, $0.6\lambda_0$ respectively). In all cases, dipole moments are oriented parallelly to the chain and intracell separations are the same ($b = 0.15\lambda_0$).

This can also be discussed in terms of crystal momentum k meaningfully by considering that in order to obtain subradiant modes, it requires the light line to lie inside the first Brillouin zone of the such that $|\frac{\pi}{a}| > |k_0| = |\pm\frac{2\pi}{\lambda_0}|$, giving $a < \frac{\lambda_0}{2}$.
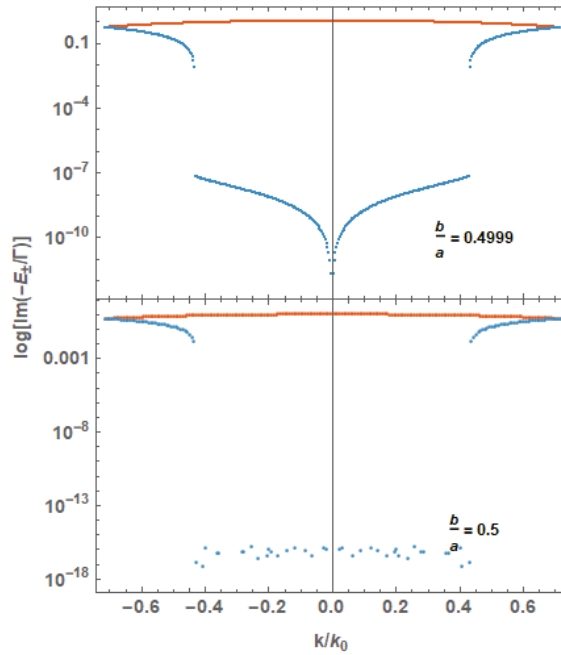
Figure 2.4: Plots of $\mathfrak{I}[E_\pm]$ in logarithmic scale for $\frac{a}{\lambda_0} = 0.7$.

Another key point to consider here, is that the one dimensional diatomic chain of interest display subradiant behavior with modes having zero decay rate depending on the length of a unit cell relative to natural wavelength and not on the atomic spacings. In

27

the upper panel of Figure 2.4 Imaginary parts of energies are plotted in logarithmic scale
for the case where interatomic spacings are less than half the wavelength, but unit cell
length is larger than the critical value ($\frac{a}{\lambda_0} = 0.7$, $\frac{b}{a} = 0.5 - 10^{-4}$). It is clear that there is
no subradiant regime for this case. The bottom row of Figure 2.4 shows the decay rates
for $\frac{a}{\lambda_0} = 0.7$ and $\frac{b}{a} = 0.5$. In this configuration, we actually have a monatomic chain
with unit cell length $0.35\lambda_0 < 0.5\lambda_0$ and as expected from Section 2.1, we indeed see
subradiant modes between $k = \pm\frac{k_0}{2}$.The reason that the period of spatial repetition plays
a crucial role suppressing the emission is that it is the states belonging to same sublattices
that interfere destructively.

2.3.2 Finite Diatomic Chain

In one excitation framework, the real space non-Hermitian tight binding Hamilto-
nian given in Equation (2.18) for a finite chain of N unit cells, has $2N$ complex eigenvalues
that are shown in Figure 2.5 for different dipole moment orientations ($\theta = 0, \arccos\frac{1}{\sqrt{3}}, \frac{\pi}{2}$)
and $\frac{a}{\lambda_0} = 0.3$. Again, the imaginary parts of the eigenvalues denote half the collective
decay rates of the corresponding eigenstates ($\mathfrak{I}[E_i] = \frac{\Gamma_i}{2}$), while the real parts are the
energies associated with them. It can be seen that, for some states, emission is extremely
suppressed. However, due to the boundaries of the chain, the decay rates of the subradiant
states are not zero, but considerably small relative to the decay rate Γ of an individual
atom.
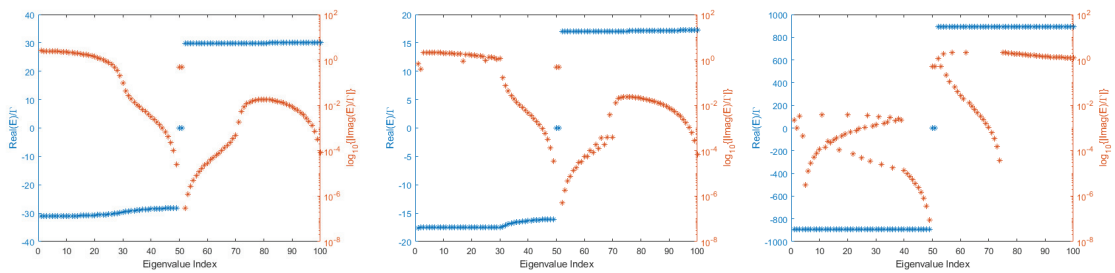
Figure 2.5: The figures are for the configurations where the dipole moments forming
the chain make an angle $\theta = 0$, $\theta = cos^{-1}(\frac{1}{\sqrt{3}})$, $\theta = \frac{\pi}{2}$ with the chain
axis respectively. The intercell and intracell separations are chosen such that
$a = 0.3\lambda_0$, $b = 0.8a$. In every plot, the number of unit cells is 50. Left vertical
axes (blue) show the real parts of energy eigenvalues and the right axes (red)
show the imaginary parts in logarithmic scale.

2.4   Topological Properties of Atomic Chain

The model considered here has some crucial distinctions with the standard SSH model that are discussed briefly in Section 1.3. Firstly, the diatomic chain of consideration is interacting with its environment and vulnerable to dissipation. Therefore, the Hamiltonian that effectively describes its dynamic is no longer Hermitian. One other distinction is that the SSH model leans on situations where only nearest-neighbor hoppings are allowed. But this model displays all-to-all hoppings between atoms with amplitudes that decay polinomially with interatomic distance, with a dominant factor $\frac{1}{r_{n\alpha;m\beta}}$. This is especially problematic for the insurance of a quantized Berry phase, since intra-sublattice hoppings may break chiral symmetry since the Hamiltonian will have non-zero diagonal elements. This, for instance, is the case for a one-dimensional diatomic lattice with nonidentical sites.

2.4.1   Infinite Chain and Calculation of Complex Berry Phase

We can see that the real and imaginary parts of $\Omega_{\alpha\beta}$ and $\Gamma_{\alpha\beta}$ are related such that;

$$
\begin{aligned}
\mathfrak{R}(\Omega_{AB}(k)) = \mathfrak{R}(\Omega_{BA}(k)) = \Omega^R, \quad \mathfrak{R}(\Gamma_{AB}(k)) = \mathfrak{R}(\Gamma_{BA}(k)) = \Gamma^R \\
\mathfrak{I}(\Omega_{AB}(k)) = -\mathfrak{I}(\Omega_{BA}(k)) = \Omega^I, \quad \mathfrak{I}(\Gamma_{AB}(k)) = -\mathfrak{I}(\Gamma_{BA}(k)) = \Gamma^I
\end{aligned}
\tag{2.26}
$$

Therefore, The effective Hamiltonian can be written as;

$$
H_k = \begin{bmatrix} G_{\alpha\alpha} & (\Omega^R + \frac{1}{2}\Gamma^I) + i(\Omega^I - \frac{1}{2}\Gamma^R) \\ (\Omega^R - \frac{1}{2}\Gamma^I) + i(-\Omega^I - \frac{1}{2}\Gamma^R) & G_{\alpha\alpha} \end{bmatrix}
\tag{2.27}
$$

$$
= G_{\alpha\alpha}\sigma_0 + (\Omega^R - \frac{i}{2}\Gamma^R)\sigma_x + (-\Omega^I - \frac{i}{2}\Gamma^I)\sigma_y = \overrightarrow{\gamma} \cdot \overrightarrow{\sigma} + G_{\alpha\alpha}\sigma_0
$$

Which lacks a term proportional to σ_z since the diagonal elements are equal. Here, the vector $\overrightarrow{\gamma}$ is defined in the same way as in Section 1.3 but its components are now complex.

29

This makes Equation (2.27) of the form;

$$H = \begin{bmatrix} G_{\alpha\alpha} & \gamma_x - i\gamma_y \\ \gamma_x + i\gamma_y & G_{\alpha\alpha} \end{bmatrix} \qquad (2.28)$$

With right eigenstates;

$$\left|\Psi_{\pm}^{R}\right\rangle = \frac{1}{\sqrt{2(\gamma_x^2 + \gamma_y^2)}} \begin{bmatrix} \gamma_x - i\gamma_y \\ \pm\sqrt{\gamma_x^2 + \gamma_y^2} \end{bmatrix} \qquad (2.29)$$

And, complex eigenvalues, $E_{\pm} = G_{\alpha\alpha} \pm \sqrt{\gamma_x^2 + \gamma_y^2}$. The left eigenvalues and eigenstates are the ones of $H^{\dagger}$.

$$\left|\Psi_{\pm}^{L}\right\rangle = \frac{1}{\sqrt{2(\gamma_x^2 + \gamma_y^2)}^{*}} \begin{bmatrix} \gamma_x^{*} - i\gamma_y^{*} \\ \pm\sqrt{\gamma_x^2 + \gamma_y^2}^{*} \end{bmatrix} \qquad (2.30)$$

And they are biorthogonal to the right states shown in Equation (2.29). Here, the star is for complex conjugation. The corresponding energy eigenvalues satisfy; $E_{\pm}^{L} = E_{\pm}^{*} = G_{\alpha\alpha}^{*} \pm \sqrt{\gamma_x^2 + \gamma_y^2}^{*}$.

The Berry phase is defined for biorthogonal basis as;

$$Q_{\pm} = \oint_{BZ} \left\langle \Psi_{\pm}^{L} \middle| \partial_k \middle| \Psi_{\pm}^{R} \right\rangle dk \qquad (2.31)$$

This is often referred to as *cBerry/complex Berry* phase.[23] To proceed, $\left|\Psi_{\pm}^{R}\right\rangle$ and, $\left|\Psi_{\pm}^{L}\right\rangle$ can be parameterized as;

$$\left|\Psi_{\pm}^{R}\right\rangle = \frac{1}{\sqrt{2cos(\frac{\alpha}{2})sin(\frac{\alpha}{2})}} \begin{bmatrix} \cos\left(\frac{\alpha}{2}\right) \\ \pm sin(\frac{\alpha}{2})e^{i\phi} \end{bmatrix} \qquad (2.32)$$

$$\left|\Psi_{\pm}^{L}\right\rangle = \frac{1}{\sqrt{2\cos\left(\frac{\alpha}{2}\right)sin(\frac{\alpha}{2})}} \begin{bmatrix} sin(\frac{\alpha}{2}) \\ \pm \cos\left(\frac{\alpha}{2}\right)e^{i\phi} \end{bmatrix} \qquad (2.33)$$

Where α and ϕ take real values and are defined such that, $\tan \alpha = \frac{|\gamma_x + i\gamma_y|}{\left|\sqrt{\gamma_x^2 + \gamma_y^2}\right|}$ and, the phase $\phi = Arg[\gamma_x + i\gamma_y] - Arg[\sqrt{\gamma_x^2 + \gamma_y^2}]$. This yields, a real valued cBerry phase;

$$Q_{\pm} = \int_{-\frac{\pi}{a}}^{\frac{\pi}{a}} \dot{\phi} \, dk \qquad (2.34)$$

The phase ϕ is plotted in first Brillouin zone for different spacings in Figure 2.6. For
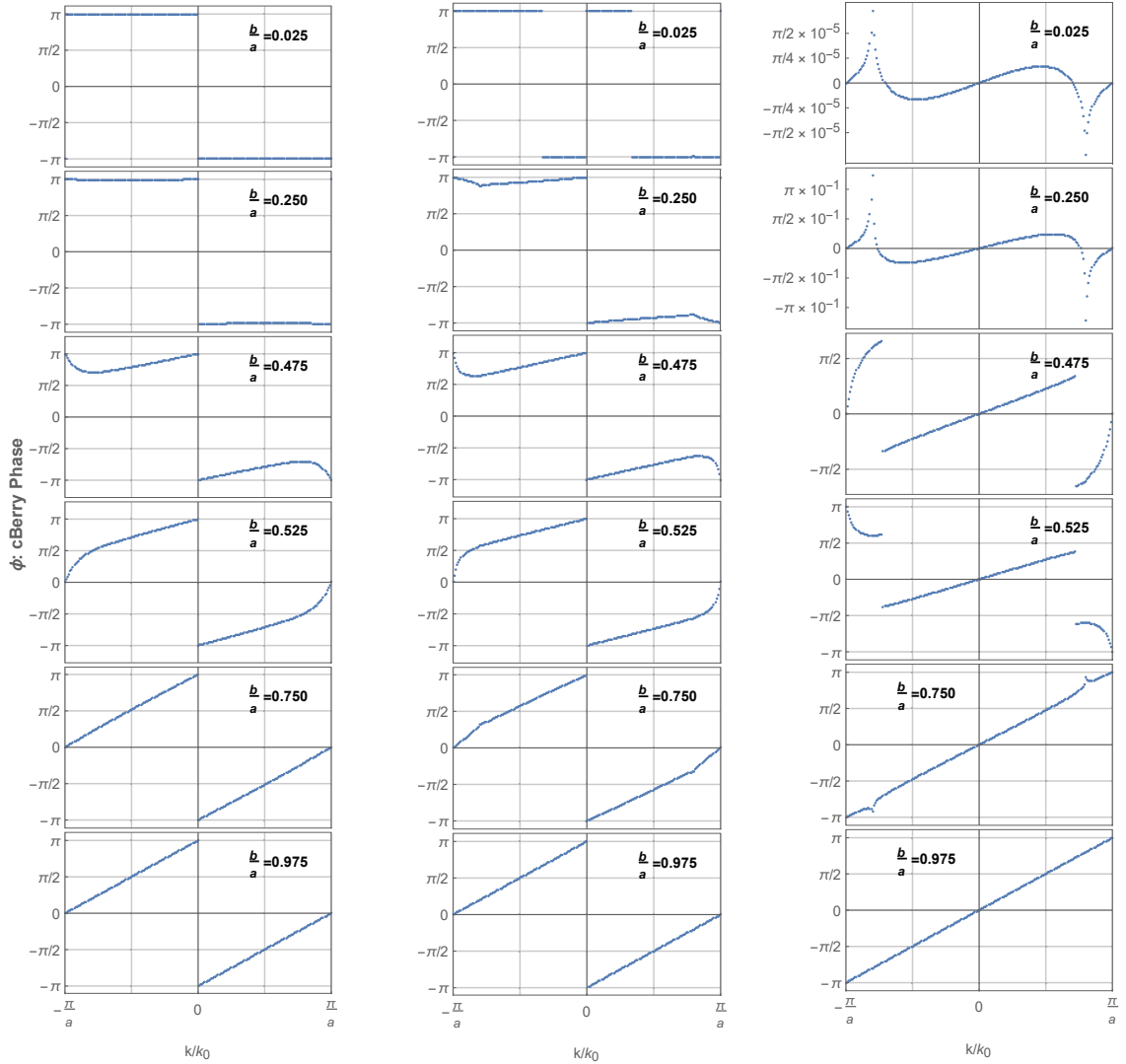
Figure 2.6: Phases φ are plotted in first Brillouin zone for different $\frac{b}{a}$ values. In left panel, the phases are plotted for parallel dipole moments, In middle and right panels, the dipole moments are perpendicular, and making an angle $\arccos \frac{1}{\sqrt{3}}$ respectively. Since for $\theta = \frac{\pi}{2}, \arccos \sqrt{1/3}$ we have singularities at $k = \pm k_0$, a Yukawa potential with $\epsilon = 0.01$ is used to alter that.

three different dipole orientations of interest. One can see from the plots that regardless of orientation of dipoles, the obtained complex Berry phases require same conditions to be nonzero over a Brillouin zone as the standard SSH model requires for non-trivial topology. We obtain the closed integral over k of $\dot{\phi}$ as zero for $b < 0.5a$ namely, intracell hopping amplitudes being greater than intercell hopping amplitudes, and nonzero for $b > 0.5a$.

2.4.2 Finite Chain and Edge States

When the eigenvalue equation is solved for real space tight binding Hamiltonian in Equation (2.18) of N unit cells, As predicted from the bulk properties, mid gap edge states arise when the distance b between two atoms in the unit cell is greater than half of the lattice parameter a. In the previous section, the mid-gap states in Figure 2.5 are the edge states and their decay rates are around that of an individual atom.
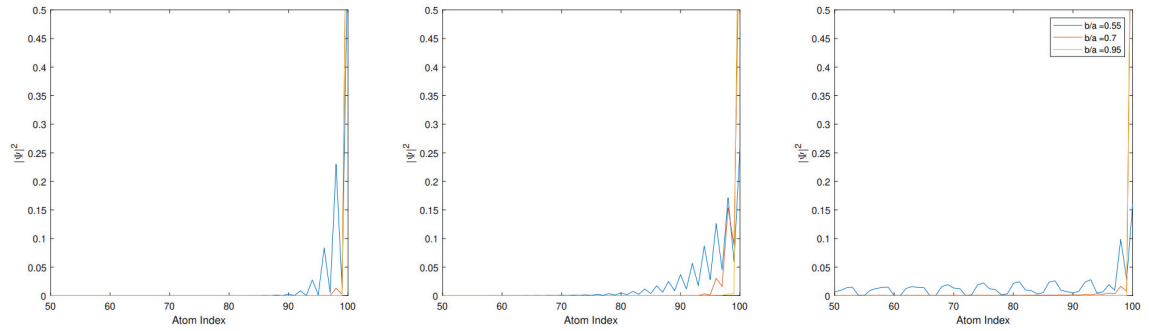
Figure 2.7: One of the two edge states of an atomic chain with 50 unit cells for different $\frac{b}{a}$ values. left, middle and right panels are for $\theta = 0, arccos\frac{1}{\sqrt{3}}, \frac{\pi}{2}$ respectively. It can be seen from figures that as b gets closer to $\frac{a}{2}$, probability distributions start to delocalize towards the bulk.

The probability distributions of the edge states are plotted in Figure 2.7. It can be seen that the states get highly localized around the boundaries of the chain as we approach fully dimerized limit, namely, as $\frac{b}{a}$ gets larger. Participation ratio (PR) can be used as a measure of localization of a state, It is usually defined as:

$$PR = \frac{1}{2N} \frac{1}{\sum_{i=1}^{2N} |\psi(r_i)|^4} \qquad (2.35)$$

Where, it measures localizations at atomic positions, and i's are over atomic indices.

A completely delocalized state $\psi(r) = \frac{1}{\sqrt{2N}}$, we would have $PR = 1$ and For a state $\psi(r) = \delta_{ij}$ that is completely localized at r_j, we would have, $PR = \frac{1}{2N}$. The participation ratios are plotted in Figure 2.8 for both trivial and topological cases. It can be seen that in topological case, the edge states do have very small participation ratios near $\frac{1}{2N}$.
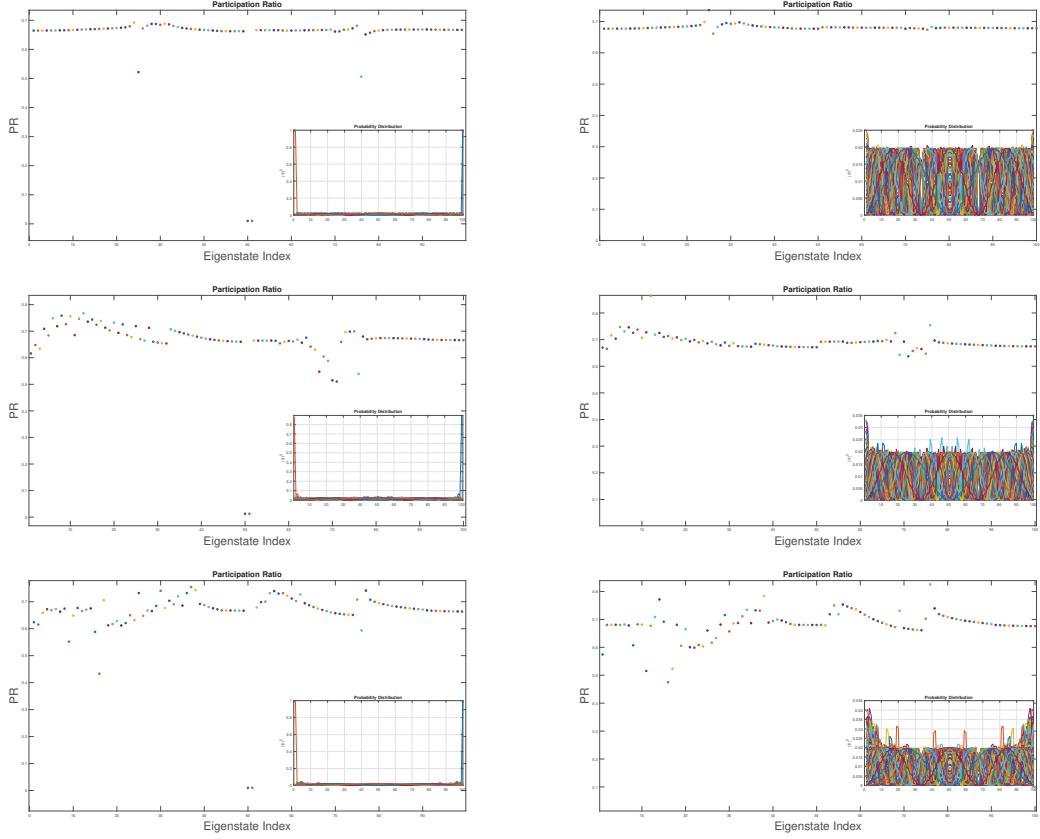
Figure 2.8: The figures show participation ratios of all states for, again $\theta = 0, arccos\frac{1}{\sqrt{3}}, \frac{\pi}{2}$ respectively from top to bottom. The insets show the probability distributiions of all states. The right panel is in topologically trivial regime with $\frac{b}{a} = 0.3$ and the left is topologically nontrivial with $\frac{b}{a} = 0.8$. In these figures, the chain has 50 unit cells..

2.5 Radiative Properties of Atomic Chain

In this chapter, the Poynting vector of the emitted radiation from different states of the atomic chain will be investigated at times much larger than the lifetime of an excitation.

In single excitation realm, the time dependent state of the whole model is,

$$|\Psi(t)\rangle = |\Psi_0(t)\rangle + |\Psi_R(t)\rangle \tag{2.36}$$

Where $|\Psi_0(t)\rangle$ is the state of the model before emission, and $|\Psi_R(t)\rangle$ is the state after the occurrence of collective emission from the chain.

$$|\Psi_0(t)\rangle = |\Psi_{at}(t)\rangle_{chain} \otimes |0\rangle_{field}$$
$$|\Psi_R(t)\rangle = |g\rangle_{chain} \otimes \left|\Psi_{ph}(t)\right\rangle_{field} \tag{2.37}$$

The initial (before de-excitation) state of the field is vacuum state $|0\rangle$, and the atomic chain is singly excited having the state $|\Psi_{at}(t)\rangle = \sum_{n\alpha} c_{n\alpha}(t)\sigma_+^{n\alpha} |g\rangle$. As before, the expression $\sigma_+^{n\alpha} |g\rangle$ is used to state that all atoms forming the chain are in their ground state except for the atom at position $\vec{r}_{n\alpha}$. Therefore, it is evident that the initial atomic state $|\Psi_{at}(t)\rangle$ is a superposition of singly excited atomic states. After the chain emits photon to the field, its state is denoted as $|g\rangle$ implying that the chain, and of course all atoms forming the chain are in ground state, in a similar manner, the field is in $\left|\Psi_{ph}(t)\right\rangle = \sum_{q\nu} c_{q\nu}(t) |1_{q\nu}\rangle$ and as in previous sections, the summation is over field modes $\vec{q}$ and polarizations ν. We can rewrite Equation (2.36) explicitly in the form:

$$|\Psi(t)\rangle = \sum_{n\alpha} c_{n\alpha}(t)\sigma_+^{n\alpha} |g\rangle \otimes |0\rangle + \sum_{q\nu} c_{q\nu}(t) |g\rangle \otimes |1_{q\nu}\rangle \tag{2.38}$$

The wavefunctions of the excited atomic systems can be found via Weisskopf-Wigner method under the same approximations that we have done.[27] Yet they are already known from previous sections, for an infinite chain of atoms, we have, $c_{n\alpha}(t) = \frac{1}{\sqrt{N}}e^{-\frac{i}{\hbar}E_k t}e^{ikna}c_{n\alpha}$, E_k's are the complex energy bands for infinite chain from section 2.2, and for finite chain, the eigenvectors and eigenvalues of effective Hamiltonian given by Equation (2.18) are found numerically obeying $c_{n\alpha}(t) = e^{-\frac{i}{\hbar}Et}c_{n\alpha}$. It is worth reminding that since the continuous evolution of the initial atomic chain is defined by the non Hermitian Hamiltonian

H_{eff}, the eigenvalues are complex. Recall the total Hamiltonian in Equation (2.9).

$$H = \sum_{n\alpha} \frac{\hbar\omega_0}{2}\sigma_z^{n\alpha} + \sum_{q\nu} \hbar\omega_q b_{q\nu}^\dagger b_{q\nu} - \sum_{\substack{q,\nu \\ n,\alpha}} g_{q\nu}(e^{i\vec{q}\cdot\vec{r}_{n\alpha}}\sigma_+^{n\alpha}b_{q\nu} + h.c). \qquad (2.39)$$

With, the local coupling constant for identical atoms, and parallel dipole moments; $g_{q\nu} = \vec{d} \cdot \vec{e}_{q\nu}\sqrt{\frac{\hbar\omega_q}{2\varepsilon_0 V}}$. Switching to interaction picture by the use of the unitary operator $\hat{U}$,

$$\hat{U} = e^{iw_0 t(\sum_{n\alpha} \frac{1}{2}\sigma_z^{n\alpha} + \sum_{q\nu} b_{q\nu}^\dagger b_{q\nu})} \qquad (2.40)$$

The transformed state vector becomes $|\Psi'\rangle = \hat{U}|\Psi\rangle$ By the use of Schrödinger equation,

$$i\hbar|\dot{\Psi}\rangle' = H'|\Psi'\rangle = i\hbar\dot{U}|\Psi\rangle + Ui\hbar|\dot{\Psi}\rangle = i\hbar\dot{U}|\Psi\rangle + UH|\Psi\rangle = H'\hat{U}|\Psi\rangle \qquad (2.41)$$

The Hamiltonian in this picture becomes

$$H' = i\hbar\dot{U}U^\dagger + UHU^\dagger \qquad (2.42)$$

Giving,

$$H' = \sum_{q\nu} \Delta_q b_{q\nu}^\dagger b_{q\nu} - \sum_{\substack{q,\nu \\ n,\alpha}} g_{q\nu}(e^{i\vec{q}\cdot\vec{r}_{n\alpha}}\sigma_+^{n\alpha}b_{q\nu} + h.c) \qquad (2.43)$$

Here, the detuning Δ_q is defined as,

$$\Delta_q = \hbar(\omega_q - \omega_0) \qquad (2.44)$$

Substituting Equations (2.43) and (2.38), into Schrödinger equation, we find the following differential equation for $c_{q\nu}$:

$$i\hbar\dot{c}_{q\nu}(t) = \Delta_q c_{q\nu}(t) - \sum_{n\alpha} g_{q\nu}e^{-i\vec{q}\cdot\vec{r}_{n\alpha}}c_{n\alpha}(t) \qquad (2.45)$$

Initially, the atomic chain is in excited state and no photon is present in reservoir. Therefore, with the initial condition $c_q(0) = 0$, Equation (2.45) is solved for the photon amplitude c_q

as:

$$c_{q\nu}(t) = \sum_{n\alpha} g_{q\nu} e^{-\vec{q}\cdot\vec{r}_{n\alpha}} \frac{e^{-\frac{i}{\hbar}Et} - e^{-\frac{i}{\hbar}\Delta_q t}}{\Delta_q - E} c_{n\alpha}(0) \tag{2.46}$$

In the limit $t \gg \frac{\hbar}{E_I}$, the time evolution of atomic system amplitudes goes to zero $e^{-\frac{i}{\hbar}Et} \to 0$. Therefore, $c_{q\nu}(t)$ can be expressed as,

$$c_{q\nu}(t) = -\sum_{n\alpha} g_{q\nu} e^{-\vec{q}\cdot\vec{r}_{n\alpha}} \frac{e^{-\frac{i}{\hbar}\Delta_q t}}{\Delta_q - E} c_{n\alpha}(0) \tag{2.47}$$

Note that at the times we considered ($t \gg \frac{\hbar}{E_I}$) we also have $|\Psi_0\rangle \to 0$. Therefore, after a time sufficiently longer than excitation lifetime, we have:

$$\left|\Psi'(t)\right\rangle = \sum_{q\nu} c_{q\nu}(t) |g\rangle |1_{q\nu}\rangle \tag{2.48}$$

Where, $|\Psi'(t)\rangle = |\Psi(t \gg \hbar/E_I)\rangle$ Now that we have all the necessary information about the total state at late times, we can investigate the directional power flow of the emitted radiaton. The Poynting vector in vacuum is

$$\vec{S} = \frac{1}{\mu_0} \left\langle : \vec{E} \times \vec{B} : \right\rangle \tag{2.49}$$

Where the expectation value is over the state at late times which is given in Equation (2.48) for large t, and vacuum contribution to the expectation value is eliminated by applying normal order. This gives an open form

$$\vec{S} = \frac{1}{\mu_0} \left\langle (\vec{E}^{(-)} \times \vec{B}^{(+)} - \vec{B}^{(-)} \times \vec{E}^{(+)}) \right\rangle \tag{2.50}$$

Where, $E^{(\pm)}$ and $B^{(\pm)}$ are the positive and negative frequency parts of electric and magnetic fields respectively, and they read:

$$\begin{aligned}
\vec{E}^{(+)} &= i\sum_{q\nu} \sqrt{\frac{\hbar\omega_q}{2\varepsilon_0 V}} b_{q\nu} e^{i\vec{q}\cdot\vec{r}} \vec{e}_{q\nu}, & \vec{E}^{(-)} &= [\vec{E}^{(+)}]^\dagger, \\
\vec{B}^{(+)} &= i\sum_{q\nu} \sqrt{\frac{\hbar}{2\varepsilon_0 V \omega_q}} b_{q\nu} e^{i\vec{q}\cdot\vec{r}} (\vec{q} \times \vec{e}_{q\nu}), & \vec{B}^{(-)} &= [\vec{B}^{(+)}]^\dagger.
\end{aligned} \tag{2.51}$$

We can use completeness relations for both system and bath, and obtain the following nonzero contributions.

$$\vec{S} = \frac{1}{\mu_0}(\langle \Psi(t)| \vec{E}^{(-)} |g\rangle |0\rangle \times \langle g| \langle 0| \vec{B}^{(+)} |\Psi(t)\rangle$$
$$- \langle \Psi(t)| \vec{B}^{(-)} |g\rangle |0\rangle \times \langle g| \langle 0| \vec{E}^{(+)} |\Psi(t)\rangle) \tag{2.52}$$

Where the last two terms are complex conjugation of the rest. From these, for instance, $\langle g| \langle 0| \vec{E}^{(+)} |\Psi'(t)\rangle$ term with positive frequency part of the electric field gives us,

$$\langle 0| \vec{E}^{(+)} \left|\Psi'(t)\right\rangle = -i \sum_{\substack{q\nu \\ n,\alpha}} \sqrt{\frac{\hbar\omega_q}{2\varepsilon_0 V}} g_{q\nu} \vec{e}_{q\nu} e^{i\vec{q}\cdot(\vec{r}-\vec{r}_{n\alpha})} e^{-\frac{i}{\hbar}\Delta_q t} \frac{c_{n\alpha}(0)}{\Delta_q - E} \tag{2.53}$$

The summation over the polarizations ν of the radiation can be taken beforehand considering that when the coupling constant for identical dipoles $g_{q\nu} = \vec{d} \cdot \vec{e}_{q\nu} \sqrt{\frac{\hbar\omega_q}{2\varepsilon_0 V}}$ is substituted, the only ν dependence is in $(\vec{d} \cdot \vec{e}_{q\nu})\vec{e}_{q\nu}$ term which is mutual for both infinite and finite chain.

$$\sum_\nu (\vec{d} \cdot \vec{e}_{q\nu})\vec{e}_{q\nu} = \sum_i \sum_j d_i(\vec{e_j}) \sum_\nu [\vec{e}_{q\nu}]_i [\vec{e}_{q\nu}]_j \tag{2.54}$$

In order to further simplify this, we can apply the fact that, since the unit vector along propagation direction $\hat{q}$, and the unit polarization vectors are orthogonal to each other, they obey completeness relation.

$$\sum_\nu [\vec{e}_{q\nu}]_i [\vec{e}_{q\nu}]_j = \delta_{ij} - [\hat{q}]_i [\hat{q}]_j \tag{2.55}$$

With the help of Equation (2.55), Equation (2.54) is simplified as

$$\sum_\nu (\vec{d} \cdot \vec{e}_{q\nu})\vec{e}_{q\nu} = \sum_i \sum_j d_i\hat{j}(\delta_{ij} - [\hat{q}]_i[\hat{q}]_j) = \sum_i d_i\hat{i} - (\sum_i d_i[\hat{q}]_i)(\sum_j [\hat{q}]_j\hat{j}) \tag{2.56}$$

Meaningly, we simplified the expression to

$$\sum_\nu (\vec{d} \cdot \vec{e}_{q\nu})\vec{e}_{q\nu} = \vec{d} - (\vec{d} \cdot \hat{q})\hat{q} \tag{2.57}$$

Since $\sum_i d_i\hat{i} = \vec{d}$, $\sum_i d_i[\hat{q}]_i = \vec{d} \cdot \hat{q}$, and $\sum_j [\hat{q}]_j\hat{j} = \hat{q}$. Substituting Equation (2.54) and

37

the coupling constant $g_{q\nu}$, Equation (2.53) becomes:

$$\langle 0| \vec{E}^{(+)} \left|\Psi'(t)\right\rangle = -i \sum_{\substack{q \\ n,\alpha}} \frac{\hbar\omega_q}{2\varepsilon_0 V} e^{i\vec{q}\cdot(\vec{r}-\vec{r}_{n\alpha})} c_{n\alpha}(0) \frac{e^{\frac{-i}{\hbar}\Delta_q t}}{\Delta_q - E} [\vec{d} - (\vec{d}\cdot\hat{q})\hat{q}] \quad (2.58)$$

2.5.1   Radiation From Infinite Chain

For infinite chain of atoms, we have $E = E_k = G_{AA} \pm \sqrt{G_{AB}G_{BA}}$ and $c_{n\alpha}(0) = \frac{1}{\sqrt{N}} e^{ikna} c_\alpha$. Therefore, Equation (2.58) reads:

$$\begin{aligned}
\langle 0| \vec{E}^{(+)} \left|\Psi'(t)\right\rangle = &\frac{-i\hbar}{\sqrt{N}2\varepsilon_0 V} \sum_n e^{i(k-q_z)na} \left(c_A + e^{-iq_z b} c_B\right)(0) \\
&\times \sum_{\vec{q}} [\vec{d} - (\vec{d}\cdot\hat{q})\hat{q}]\, \omega_q\, e^{i\vec{q}\cdot\vec{r}} \frac{e^{\frac{-i}{\hbar}\Delta_q t}}{\Delta_q - E_k}
\end{aligned} \quad (2.59)$$

Where we exploited the fact that $\vec{q}\cdot\vec{r}_{n\alpha} = q_z r_{n\alpha}$. And notice that we took the summation over α is also taken:

$$\sum_\alpha e^{-i\vec{q}\cdot\vec{r}_{n\alpha}} c_\alpha(0) = e^{-iq_z na}\left(c_A + e^{-iq_z b} c_B\right) \quad (2.60)$$

And, $\vec{d}_{n\alpha} = \vec{d}_{m\beta} = \vec{d}$. While moving to the continuum limit, we can impose the periodicity along along z on $\vec{q}$.

$$\sum_{\vec{q}} \to \frac{A}{(2\pi)^2} \sum_{q_z} \iint q_\perp dq_\perp d\varphi \quad (2.61)$$

Where, q_z is the component of the photon momentum in the parallel direction to the chain, $q_\perp$ is the component in the radial direction and the azimuth φ is the angle that $\vec{q}$ makes with the chain. In Equation (2.59), we can easily carry out the summation over the unit cells;

$$\sum_n e^{i(k-q_z)na} = N\delta_{k,q_z} \quad (2.62)$$

Restricting the component of photon momentum on chain direction to k. Substitution yields:

$$\langle 0| \vec{E}^{(+)} |\Psi'(t)\rangle = \frac{-i\hbar A\sqrt{N}}{(2\pi)^2 2\varepsilon_0 V} \sum_{q_z,\alpha} (c_A + e^{-iq_z b}c_B)(0)\, \delta_{k,q_z}$$
$$\times \iint [\vec{d} - (\vec{d} \cdot \hat{q})\hat{q}]\, \omega_q\, q_\perp\, e^{i\vec{q}\cdot\vec{r}}\, \frac{e^{\frac{-i}{\hbar}\Delta_q t}}{\Delta_q - E_k}\, dq_\perp\, d\varphi \tag{2.63}$$

And $\frac{A}{V} = \frac{1}{L}$ where L is the normalization length. At this step, I will take the summation over q_z making $q = \sqrt{q_\perp^2 + k^2}$. However, I will not change the notation and denote it as q. Therefore, it is useful to keep in mind that q_z is constant and equals to the crystal momentum k.

$$\langle 0| \vec{E}^{(+)} |\Psi'(t)\rangle = \frac{-i\hbar\sqrt{N}}{(2\pi)^2 2\varepsilon_0 L} (c_A + e^{-ikb}c_B)$$
$$\times \iint [\vec{d} - (\vec{d} \cdot \hat{q})\hat{q}]\, \omega_q\, q_\perp\, e^{i\vec{q}\cdot\vec{r}}\, \frac{e^{\frac{-i}{\hbar}\Delta_q t}}{\Delta_q - E_k}\, dq_\perp\, d\varphi \tag{2.64}$$

The integration over the azimuthal angle φ of the radiation can be isolated as,

$$\int_0^{2\pi} [\vec{d} - (\vec{d} \cdot \hat{q})\hat{q}]e^{i\vec{q}\cdot\vec{r}}d\varphi \tag{2.65}$$

The integral in Equation (2.65) is a Laplace integral with a pure imaginary phase. Since the integral has a rapidly oscillating exponential, one can apply the method of stationary phase, stating that the most contribution will come from the neighborhood of the stationary point of the phase.[32] Stationary point of the phase is where $\cos\varphi$ has its maximum which corresponds to the situation where the azimuths of $\vec{q}$ and $\vec{r}$ are the same. Therefore, we have;

$$\int_0^{2\pi} [\vec{d} - (\vec{d} \cdot \hat{q})\hat{q}]e^{i\vec{q}\cdot\vec{r}}d\varphi \approx f(q_\perp)e^{ikz}\sqrt{\frac{2\pi}{\rho q_\perp}}[e^{i\rho q_\perp - i\frac{\pi}{4}} + e^{-i\rho q_\perp + i\frac{\pi}{4}}]$$
$$\approx 2\pi f(q_\perp)e^{ikz} J_0(\rho q_\perp) \tag{2.66}$$

Where, $f(q_\perp) = \vec{d} - (\vec{d} \cdot \hat{q})\hat{q}$ and ρ is the radial distance from the chain. We also have $\sqrt{\frac{2\pi}{q_\perp \rho}}[e^{i\rho q_\perp - i\frac{\pi}{4}} + e^{-iq_\perp\rho + i\frac{\pi}{4}}] = 2\pi(H_0^{(1)} + H_0^{(2)}) = 2\pi J_0(\rho q_\perp)$. Where $J_p(\rho q_\perp)$ is Bessel function of first kind, and, $H_p^{(1)}$, $H_p^{(2)}$ Denotes Hankel functions of the first and second kinds respectively. With asymptotic forms $H_p^{(1)}(z) = \sqrt{\frac{2}{\pi z}}e^{i(z - \frac{\pi}{2}p - \frac{\pi}{4})}$, and,

$H_p^{(2)}(z) = \sqrt{\frac{2}{\pi z}} e^{-i(z - \frac{\pi}{2} p - \frac{\pi}{4})}$. Substituting what we have in hand, we obtain

$$\langle 0 | \vec{E}^{(+)} | \Psi'(t) \rangle = \frac{-i\hbar\sqrt{N}}{L(4\pi)\varepsilon_0} (c_A + e^{-ikb} c_B) e^{ikz}$$
$$\times \int_0^\infty q_\perp \omega_q [\vec{d} - (\vec{d} \cdot \hat{q})\hat{q}] e^{-i\omega_q t} \frac{J_p(\rho q_\perp)}{\Delta_q - E_k} dq_\perp \qquad (2.67)$$

Where, now, after summation over n, and integration over φ, the z component of $\vec{q}$ is fixed as k, and the radial direction of $\hat{q}$ is fixed to the radial direction $\hat{\rho}$ of the position vector $\vec{r}$,. In order to determine the final expression for (2.53), we are only left with the integration over radial component of $\vec{q}$. The lower limit of the integral can be extended without worrying about the signs of exponential $\pm\frac{\pi}{4}$ terms, since their sign will be taken care of by $sgn(-q_\perp\rho)$ coming from the stationary phase method. And, we can make narrow band approximation $q \approx q_0'$ with $\hbar\omega_q = \Re[E_k] + \hbar\omega_0 = \hbar c q_0'$ considering that the imaginary parts of energies are relatively small and, $q_\perp^2 \approx q_0'^2 - k^2$ for non-oscillatory terms except from the one in denominator.

$$\langle g | \langle 0 | \vec{E}^{(+)} | \Psi'(t) \rangle = \frac{-i\hbar c\sqrt{N}}{L(4\pi)\varepsilon_0} (c_A + e^{-ikb} c_B) e^{ikz} \sqrt{\frac{2}{\pi\rho\sqrt{q_0'^2 - k^2}}}$$
$$\times \sum_\alpha (q_0'^2 - k^2)[\vec{d} - (\vec{d} \cdot \hat{q})\hat{q}] \qquad (2.68)$$
$$\times \int_{-\infty}^\infty dq_\perp e^{-i\omega_q t} \frac{e^{i(\rho q_\perp - \frac{\pi}{4})} + e^{-i(\rho q_\perp - \frac{\pi}{4})}}{\Delta_q - E_k}$$

This approximation we made is valid since we applied the rotating wave approximation, we are imposing that the spectral width of emitted light is narrow around a mean frequency cq_0', i.e. the amplitude C_q is non-zero only inside the range $\Delta\omega$, which is small compared to the mean photon frequency of emitted light. $|\omega_k - cq_0'| \backsim \Delta\omega \ll cq_0'$.[33][34] Poles of the integral over $q_\perp$ in Equation (2.68) is at $q_\perp = q_0^\perp$ where, $q_0 := \frac{1}{\hbar c}(E_k + \hbar\omega_0)$ and, $(q_0^\perp)^2 + k^2 = (q_0)^2$, since $\Im[E_k]$ is always negative, there is no pole in the upper half plane. For the first exponential term, we can close the contour from the lower half-plane. However, for the term including Hankel function of second kind, since $r + ct$ is always positive, we obtain exponential growth in lower half-plane, we need to close the contour from upper half plane and the result of the integration is zero. Embedding the constant $e^{-i\frac{\pi}{4}}$ terms into coefficients c_α, this gives:

$$\int_{-\infty}^\infty dq_\perp \frac{1}{\Delta_q - E_k} (e^{i(\rho q_\perp - \frac{\pi}{4})} + e^{-i(\rho q_\perp - \frac{\pi}{4})}) e^{-i\omega_q t}$$
$$= \frac{2\pi i}{\hbar c} e^{-iq_0 ct + (\rho q_0^\perp)} \theta(t - \frac{\rho}{c}) \qquad (2.69)$$

The Heaviside step function $\theta(t - \frac{\rho}{c})$ comes from the fact that for $\rho > ct$, we should close the contour in the upper half plane obtaining zero since there is no pole. And it also takes care of the fact that at time t, physically, the radiation cannot be found at positions $\rho > ct$. Gathering all together, we have, for Equation (2.53),

$$\langle g| \langle 0| \vec{E}^{(+)} \left| \Psi'(t) \right\rangle = \frac{\sqrt{N}}{L 2 \varepsilon_0} \sqrt{\frac{2}{\pi \rho}} (q_0'^2 - k^2)^{\frac{3}{4}} [\vec{d} - (\vec{d} \cdot \hat{q}) \hat{q}] (c_A + e^{-ikb} c_B)$$
$$\times e^{i(-q_0 ct + \rho q_0^\perp + kz)} \theta(t - \frac{\rho}{c}) \quad (2.70)$$

Again, I used the notation: $\hbar c q_0' = \Re[E_k] + \hbar \omega_0$ coming from narrow band approximation, $q_0 = \frac{1}{\hbar c}(E_k + \hbar \omega_0)$ and $(q_0^\perp)^2 + k^2 = q_0^2$ coming from the contour integration.

In a similar fashion, the positive frequency magnetic field term gives,

$$\left\langle \Psi'(t) \right| \vec{B}^{(-)} |g\rangle |0\rangle = \frac{\sqrt{N}}{L 2 \varepsilon_0 c} \sqrt{\frac{2}{\pi \rho}} (q_0'^2 - k^2)^{\frac{3}{4}} [\hat{q} \times \vec{d}] (c_A + e^{ikb} c_B)$$
$$\times e^{-i(-q_0^* ct + \rho q_0^{\perp *} + kz)} \theta(t - \frac{\rho}{c}) \quad (2.71)$$

This makes the Poynting vector introduced in Equation (2.49) lie along $\hat{q}$:

$$\vec{S} = \frac{1}{\mu_0} \langle \Psi(t)| \vec{E}^{(-)} |g\rangle |0\rangle \times \langle g| \langle 0| \vec{B}^{(+)} |\Psi(t)\rangle + h.c. \quad (2.72)$$

2.5.2   Radiation From A Finite Chain

For a finite chain, after the summation over field polarizations is taken, Equation (2.58) is,

$$\langle 0| \vec{E}^{(+)} \left| \Psi'(t) \right\rangle = -i \sum_{\substack{q \\ n,\alpha}} \frac{\hbar \omega_q}{2 \varepsilon_0 V} e^{i \vec{q} \cdot (\vec{r} - \vec{r}_{n\alpha})} c_{n\alpha}(0) \frac{e^{\frac{-i}{\hbar} \Delta_q t}}{\Delta_q - E} [\vec{d} - (\vec{d} \cdot \hat{q}) \hat{q}] \quad (2.73)$$

An important remark is that the indices $n\alpha$ in complex energies $E_{n\alpha}$ do not correspond to atoms at unit cell n sublattice α instead, $E_{n\alpha}$ are the eigenvalues of tight binding Hamiltonian in Equation (2.18) that correspond to state with amplitude $c_{n\alpha}$ out of $2N$ eigenvalues and eigenvectors. We can define the distance from atom at position $\vec{r}_{n\alpha}$ to the point of consideration as $\vec{\tau}_{n\alpha} = \vec{r} - \vec{r}_{n\alpha}$ beforehand. And an important distinction from above calculations is that since the chain is now finite, the cylindrical symmetry is

broken and we cannot impose periodic boundary conditions in any direction for $\vec{q}$. We no longer have the advantage to take n summation beforehand to restrict the z direction of photon momentum to k. To proceed with the summation over $\vec{q}$, we have:

$$\sum_{\vec{q}} \rightarrow \frac{V}{(2\pi)^3} \int q^2 dq d\Omega \tag{2.74}$$

In continuum limit. This makes Equation (2.73):

$$\langle 0| \vec{E}^{(+)} |\Psi'(t)\rangle = -i\frac{\hbar}{2\varepsilon_0(2\pi)^3} \sum_{n,\alpha} c_{n\alpha}(0) \int q^2\, \omega_q\, e^{i\vec{q}\cdot\vec{\imath}_{n\alpha}} [\vec{d} - (\vec{d}\cdot\hat{q})\hat{q}]$$
$$\times \frac{e^{-\frac{i}{\hbar}\Delta_q t}}{\Delta_q - E_{n\alpha}}\, dq\, d\Omega \tag{2.75}$$

Where, again, $\vec{\imath}_{n\alpha} = \vec{r} - \vec{r}_{n\alpha}$ is the distance between the point of interest, and the atom at position $\vec{r}_{n\alpha}$. The integral over the solid angle Ω can be isolated as follows.

$$\int e^{i\vec{q}\cdot\vec{\imath}_{n\alpha}} [\vec{d} - (\vec{d}\cdot\hat{q})\hat{q}]\, d\Omega \tag{2.76}$$

Performing Stationary phase approximation for integration over the solid angle Ω, where, the stationary point occurs when $\vec{q} \,\| \,\hat{\imath}_{n\alpha}$ we obtain:

$$\int e^{i\vec{q}\cdot\vec{\imath}_{n\alpha}} [\vec{d} - (\vec{d}\cdot\hat{q})\hat{q}]\, d\Omega = \frac{2\pi}{iq\imath_{n\alpha}} (e^{iq\imath} - e^{-iq\imath})[\vec{d} - (\vec{d}\cdot\hat{\imath}_{n\alpha})\hat{\imath}_{n\alpha}] \tag{2.77}$$

Substitution gives:

$$\langle 0| \vec{E}^{(+)} |\Psi'(t)\rangle = -\frac{\hbar}{2\varepsilon_0(2\pi)^2} \sum_{n,\alpha} \frac{1}{\imath_{n\alpha}} c_{n\alpha}(0) [\vec{d} - (\vec{d}\cdot\hat{\imath}_{n\alpha})\hat{\imath}_{n\alpha}]$$
$$\times \int q\,\omega_q \frac{(e^{iq\imath} - e^{-iq\imath})e^{-\frac{i}{\hbar}\Delta_q t}}{\Delta_q - E_{n\alpha}}\, dq \tag{2.78}$$

Again, applying the narrow band approximation, we have for $\hbar\omega_q = E_R - \hbar\omega_0 = \hbar c q_0'$,

$$\langle 0| \vec{E}^{(+)} |\Psi'(t)\rangle = -\frac{\hbar c}{2\varepsilon_0(2\pi)^2} \sum_{n,\alpha} \frac{1}{\imath_{n\alpha}} c_{n\alpha}(0) [\vec{d} - (\vec{d}\cdot\hat{\imath}_{n\alpha})\hat{\imath}_{n\alpha}]$$
$$\times q_0'^2 \int_0^\infty \frac{(e^{iq\imath} - e^{-iq\imath})e^{-\frac{i}{\hbar}\Delta_q t}}{\Delta_q - E_{n\alpha}}\, dq \tag{2.79}$$

42

In remaining integral, the $e^{i\omega_0 t}\int_0^\infty e^{-iq(\imath_{n\alpha}+ct)}dq \to 0$ since always $\imath_{n\alpha} + ct > 0$. and in the q integral we can extend the lower limit to infinity as before. Remaining expression has a pole at $q = \frac{1}{\hbar c}(\hbar\omega_0 + \mathfrak{R}[E_{n\alpha}] + i\mathfrak{I}[E_{n\alpha}]) = q_0$ which is always in the lower half plane since $\mathfrak{I}[E_{n\alpha}] < 0$. As discussed above while considering an infinite chain, using the residue theorem, we obtain:

$$\int_{-\infty}^{\infty} \frac{e^{iq(\imath_{n\alpha}-ct)}}{\Delta_q - E_{n\alpha}}\, dq = \frac{2\pi i}{\hbar c}e^{iq_0(\imath_{n\alpha}-ct)}\theta(ct - \imath_{n\alpha}) \tag{2.80}$$

Gathering these, we obtain the following.

$$\langle 0|\,\vec{E}^{(+)}\,\big|\Psi'(t)\big\rangle = -\frac{i\hbar}{4\pi\varepsilon_0}\sum_{n,\alpha}\frac{1}{\imath_{n\alpha}}c_{n\alpha}(0)\left[\vec{d} - (\vec{d}\cdot\hat{\imath}_{n\alpha})\hat{\imath}_{n\alpha}\right]$$
$$\times\, q_0'^2 e^{iq_0(\imath_{n\alpha}-ct)}\theta(ct - \imath_{n\alpha}) \tag{2.81}$$

Simplifying the expression using BAC-CAB $[\vec{d} - (\vec{d}\cdot\hat{\imath}_{n\alpha})\hat{\imath}_{n\alpha}] = [\vec{d}(\hat{\imath}_{n\alpha}\cdot\hat{\imath}_{n\alpha}) - (\vec{d}\cdot\hat{\imath}_{n\alpha})\hat{\imath}_{n\alpha}] = \hat{\imath}_{n\alpha}\times(\vec{d}\times\hat{\imath}_{n\alpha})$, we have:

$$\langle 0|\,\vec{E}^{(+)}\,\big|\Psi'(t)\big\rangle = -\frac{i\hbar}{4\pi\varepsilon_0}\sum_{n,\alpha}\frac{1}{\imath_{n\alpha}}c_{n\alpha}(0)\,(\hat{\imath}_{n\alpha}\times(\vec{d}\times\hat{\imath}_{n\alpha}))$$
$$\times\, q_0'^2 e^{iq_0(\imath_{n\alpha}-ct)}\theta(ct - \imath_{n\alpha}) \tag{2.82}$$

Similarly, $\vec{B}^{(-)}$ term gives,

$$\langle\Psi(t)|\,\vec{B}^{(-)}\,|g\rangle\,|0\rangle = \frac{i\hbar}{4\pi\varepsilon_0 c}\sum_{n,\alpha}\frac{1}{\imath_{n\alpha}}c_{n\alpha}(0)\,(\hat{\imath}_{n\alpha}\times\vec{d})$$
$$\times\, q_0'^2 e^{-iq_0^*(\imath_{n\alpha}-ct)}\theta(ct - \imath_{n\alpha}) \tag{2.83}$$

And the Poynting vector in Equation (2.49) as:

$$\vec{S} = \frac{1}{\mu_0}\langle\Psi(t)|\,\vec{E}^{(-)}\,|g\rangle\,|0\rangle \times \langle g|\,\langle 0|\,\vec{B}^{(+)}\,|\Psi(t)\rangle + h.c. \tag{2.84}$$

Figure 2.9, The Poynting vectors of radiation from states with different characteristics are visualized in the $x - z$ plane for a finite chain of 50 unit cells in the radiation zone at $t \gg \frac{1}{\mathfrak{I}(E)}$. The chain lies between $z = -7.62$ and $z = 7.62$, lattice parameter is taken as $0.3\lambda_0$, and the intacell separation is $0.8a$. Since the chain lies along z axis ($x = 0$, $y = 0$),

to avoid taking the plane in which the chain lies on, there is an offset by $y = 5a$ in figures. In all plots, $t = 10\omega_0 \frac{\Gamma}{E_I}$ except from the most radiant state of the chain with $\theta = \frac{\pi}{2}$ for which, the radiation is illustrated at $t = 50\omega_0 \frac{\Gamma}{E_I}$. The bottom row of the figure shows the directional power flow from the most subradiant state for the three angles of consideration in logarithmic scale. It most clearly reveals for dipoles oriented parallelly to the chain that the emission from the subradiant state is significantly suppressed in the radial direction of the alignment of the chain. Implying that, the emission occurs from the ends of the finite chain, and it is suppressed from the bulk. However, it is less clear to see for other alignments. In the central row, emission from the state with the shortest lifetime is shown to be dominant in the direction radial to the bulk of the chain, except for $\theta = \frac{\pi}{2}$, since the radial direction is also the direction of the dipole moments. Plots in the top row are for edge states localized at one end of the finite chain. Notice that they display a radiation pattern similar to that of individual dipoles, given the dipole moment orientations. It was also shown in Section 2.3.2 that decay rates of the edge states were close to single atom decay rate.
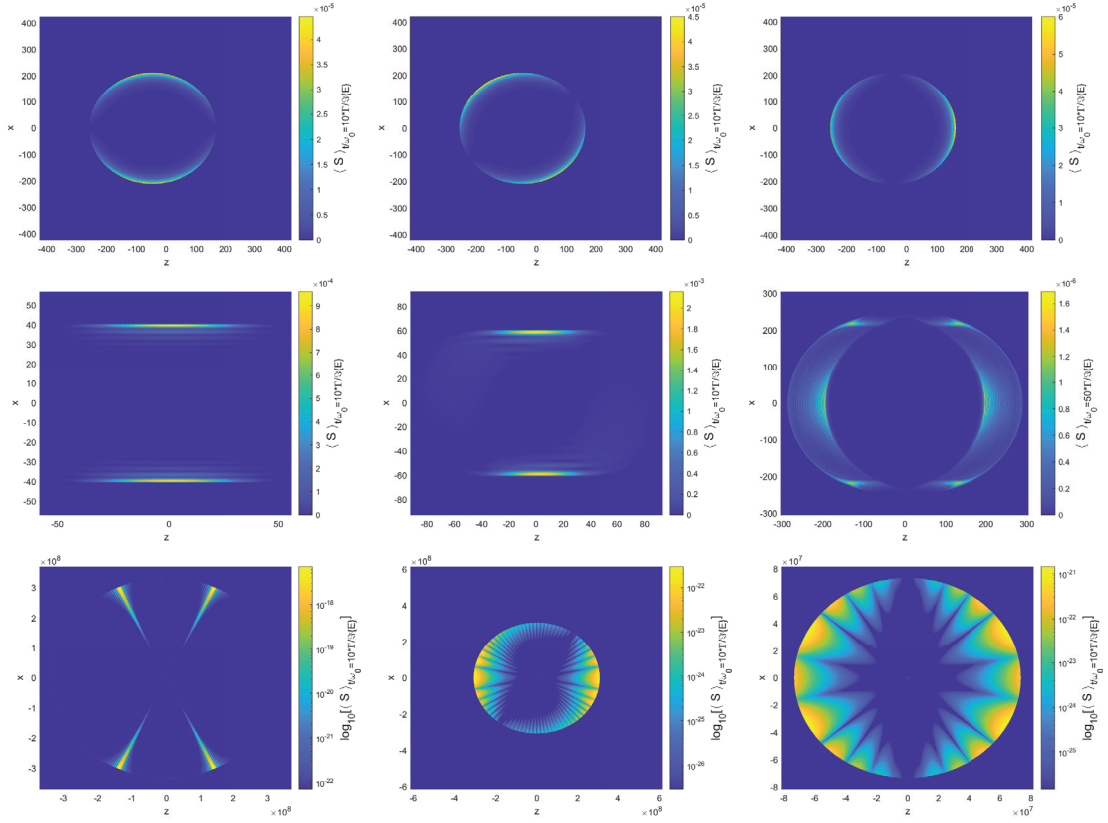
Figure 2.9: The figures in the right column are for the configurations where the dipole moments forming the chain are parallel to chain direction ($\vec{d}/\!\!/\hat{z}, \theta = 0$). figures in the central column are for $\theta = \arccos\left(1/\sqrt{3}\right)$, and in the left column, $\vec{d} \perp \hat{z}$ ($\theta = \frac{\pi}{2}$), the intercell and intracell separations are chosen such that $a = 0.3\lambda_0$, $b = 0.8a$. In every plot, the number of unit cells is 50, the chain lies on z axis. And the Poynting vector is plotted at around $\frac{t}{\omega_0} = 10\frac{\Gamma}{E_I}$ except for the most radiant state of perpendicular dipoles, Poynting vector from this state is demonstrated at $\frac{t}{\omega_0} = 50\frac{\Gamma}{E_I}$. The dipole moments lie on $x - z$ plane in every case. And the rows are for states with different properties. The top row shows one of the edge states for each situation, the middle row shows the most radiant states, and the bottom row shows radiation for subradiant states in logarithmic scale.

CHAPTER 3

CONCLUSION

In this thesis, the topological and radiative behaviors of a one-dimensional diatomic chain immersed in vacuum field is investigated. Radiative properties of the model are discussed via the decay rates obtained from the complex eigenvalues of effective non-Hermitian Hamiltonian describing the interacting system with a fixed excitation number. It is shown for a singly excited infinite chain with two identical atoms per unit cell that radiative dark states arise when the lattice constant is smaller than half the resonant wavelength of the atoms. It is shown that the same condition applies for a finite chain to have subradiant states with decay rates close to zero. However, decay rates of these states remain nonzero because of finite-size effects.

The presence of dissipation and vacuum mediated long range hoppings distinguishes the system of interest from the standard SSH model. However, for obtaining a topologically non-trivial phase, the criteria are shown to be the same as SSH model. For this model, the hopping amplitudes depend only on the atomic spacings. When the intracell hopping amplitudes are smaller than the intercell hopping amplitudes, the chain exhibits non-trivial topology and this occurs when $\frac{b}{a} < 0.5$. The Hamiltonian that effectively describes open system dynamics of consideration is non-Hermitian, so orthogonality of eigenstates are not guaranteed anymore. Therefore, the bulk boundary correspondence is shown on a biorthogonal basis, using the complex Berry phase. In real space, the mid-gap edge states are shown to highly localize at the edges as the intracell separation gets larger compared to half the unit cell length. The radiative decay rates of these localized states are close to that of an individual atom.

When the dipoles are aligned parallel to the chain, radiation in radial direction is suppressed for subradiant states, while the intensity of radiation from states with largest decay rates is highest in the radial direction. On the other hand, the edge states display a radiation pattern similar to that of a single dipole radiation.

REFERENCES

1. Dicke, R. H.; Physical, P.; Aboratory, I. Coherence in Spontaneous Radiation Processes. *Physical Review* **1954**, *93*, 99.

2. Rehler, N. E.; Eberly, J. H. Superradiance. *Physical Review A* **1971**, *3*, 1735.

3. Lehmberg, R. H. Radiation from an N-atom system. I. General formalism. *Physical Review A* **1970**, *2*, 883–888.

4. Gross, M.; Haroche, S. Superradiance: An essay on the theory of collective spontaneous emission. *Physics Reports* **1982**, *93*, 301–396.

5. Ficek, Z.; Tanaś, R. Entangled states and collective nonclassical effects in two-atom systems. *Physics Report* **2002**, *372*, 369–443.

6. Zhang, Y. X.; Mølmer, K. Theory of Subradiant States of a One-Dimensional Two-Level Atom Chain. *Physical Review Letters* **2019**, *122*, 203605.

7. Zhang, Y. X.; Mølmer, K. Subradiant Emission from Regular Atomic Arrays: Universal Scaling of Decay Rates from the Generalized Bloch Theorem. *Physical Review Letters* **2020**, *125*, 253601.

8. Facchinetti, G.; Jenkins, S. D.; Ruostekoski, J. Storing Light with Subradiant Correlations in Arrays of Atoms. *Physical Review Letters* **2016**, *117*, 243601.

9. Kalachev, A. Quantum storage on subradiant states in an extended atomic ensemble. *Physical Review A - Atomic, Molecular, and Optical Physics* **2007**, *76*, 043812.

10. Asenjo-Garcia, A.; Moreno-Cardoner, M.; Albrecht, A.; Kimble, H. J.; Chang, D. E. Exponential improvement in photon storage fidelities using subradiance "selective radiance" in atomic arrays. *Physical Review X* **2017**, *7*, 1–36.

11. Cech, M.; Lesanovsky, I.; Olmos, B. Dispersionless subradiant photon storage in one-dimensional emitter chains. *Physical Review A* **2023**, *108*, L051702.

12. Rui, J.; Wei, D.; Rubio-Abadal, A.; Hollerith, S.; Zeiher, J.; Stamper-Kurn, D. M.; Gross, C.; Bloch, I. A subradiant optical mirror formed by a single structured atomic layer. *Nature 2020 583:7816* **2020**, *583*, 369–374.

13. Henriet, L.; Douglas, J. S.; Chang, D. E.; Albrecht, A. Critical open-system dynamics in a one-dimensional optical-lattice clock. *Physical Review A* **2019**, *99*, 023802.

14. Masson, S. J.; Asenjo-Garcia, A. Atomic-waveguide quantum electrodynamics. *Physical Review Research* **2020**, *2*, 043213.

15. Tiranov, A.; Angelopoulou, V.; van Diepen, C. J.; Schrinski, B.; Sandberg, O. A. D.; Wang, Y.; Midolo, L.; Scholz, S.; Wieck, A. D.; Ludwig, A.; Sørensen, A. S.; Lodahl, P. Collective super- and subradiant dynamics between distant optical quantum emitters. *Science* **2023**, *379*, 389–393.

16. Gonzalez-Tudela, A.; Martin-Cano, D.; Moreno, E.; Martin-Moreno, L.; Tejedor, C.; Garcia-Vidal, F. J. Entanglement of two qubits mediated by one-dimensional plasmonic waveguides. *Physical Review Letters* **2011**, *106*, 020501.

17. Solano, P.; Barberis-Blostein, P.; Fatemi, F. K.; Orozco, L. A.; Rolston, S. L. Super-radiance reveals infinite-range dipole interactions through a nanofiber. *Nature Communications 2017 8:1* **2017**, *8*, 1–7.

18. Loo, A. F. V.; Fedorov, A.; Lalumiere, K.; Sanders, B. C.; Blais, A.; Wallraff, A. Photon-mediated interactions between distant artificial atoms. *Science* **2013**, *342*, 1494–1496.

19. Wang, Y.; Xu, H.; Deng, X.; Liew, T. C.; Ghosh, S.; Xiong, Q. Topological single-photon emission from quantum emitter chains. *npj Quantum Information 2024 10:1* **2024**, *10*, 1–9.

20. Lang, N.; Büchler, H. P. Topological networks for quantum communication between distant qubits. *npj Quantum Information 2017 3:1* **2017**, *3*, 1–10.

21. D'angelis, F. M.; Pinheiro, F. A.; Guéry-Odelin, D.; Longhi, S.; Impens, F. Fast and robust quantum state transfer in a topological Su-Schrieffer-Heeger chain with next-to-nearest-neighbor interactions. *Physical Review Research* **2020**, *2*, 033475.

22. Su, W. P.; Schrieffer, J. R.; Heeger, A. J. Solitons in Polyacetylene. *Physical Review Letters* **1979**, *42*, 1698.

23. Lieu, S. Topological phases in the non-Hermitian Su-Schrieffer-Heeger model. *Physical Review B* **2018**, *97*, 1–7.

24. Breuer, H.-P.; Petruccione, F. *The Theory of Open Quantum Systems*; Oxford University Press, 2007.

25. Redfield, A. G. The Theory of Relaxation Processes. *Advances in Magnetic and Optical Resonance* **1965**, *1*, 1–32.

26. Manzano, D. A short introduction to the Lindblad master equation. *AIP Advances* **2020**, *10*.

27. Barnett, S.; Radmore, P. Oxford Scholarship Online Methods in Theoretical Quantum Optics. **2017**,

28. Orszag, M. Quantum optics: Including noise reduction, trapped ions, quantum trajectories, and decoherence, third edition. *Quantum Optics: Including Noise Reduction, Trapped Ions, Quantum Trajectories, and Decoherence, Third Edition* **2016**, 1–485.

29. Daley, A. J. Quantum trajectories and open many-body quantum systems. *Advances in Physics* **2014**, *63*, 77–149.

30. Peierls, R. E.; Peierls, R. E. Oxford Scholarship Online Quantum Theory of Solids. **2007**, 1–17.

31. Shen, S.-Q. Topological Insulators. **2017**, *187*.

32. Bender, C. M.; Boettcher, S. Real Spectra in Non-Hermitian Hamiltonians Having PT Symmetry. *Physical Review Letters* **1998**, *80*, 5243.

33. Fedorov, M. V.; Efremov, M. A.; Kazakov, A. E.; Chan, K. W.; Law, C. K.; Eberly, J. H. Spontaneous emission of a photon: wave-packet structures and atom-photon entanglement. *Phys. Rev.* **2005**, *72*, 032110.

34. Rzazewski, K.; Zakowicz, W. Spontaneous emission from an extended wavepacket. *Journal of Physics B: Atomic, Molecular and Optical Physics* **1992**, *25*, L319.